A global streamflow indices time series dataset for large-sample hydrological analyses on streamflow regime (until 2022~~1~~)

Xinyu Chen[1], Liguang Jiang[1], Yuning Luo[2], and Junguo Liu[1, 3]

[1] School of Environmental Science and Engineering, Southern University of Science and Technology, Shenzhen, 518055, China

[2] State Key Laboratory of Hydrology-Water Resources and Hydraulic Engineering, and College of Hydrology and Water Resources, Hohai University, Nanjing, 210098, China

[3] Henan Provincial Key Lab of Hydrosphere and Watershed Water Security, North China University of Water Resources and Electric Power, Zhengzhou, 450046, China

Correspondence: Liguang Jiang (jianglg@sustech.edu.cn)

Abstract. With the booming big data techniques, large-sample hydrological analysis on streamflow regime is becoming feasible, which could derive robust conclusions on hydrological processes from a big-picture perspective. However, there is a lack of ~~not~~ a comprehensive global large-sample dataset for components of the streamflow regime yet. This paper presents a new time series dataset on global streamflow indices calculated from daily streamflow records after data quality control. The dataset contains 79 indices over seven major components of streamflow regime (*i.e.*, magnitude, frequency, duration, changing rate, timing, variability, and recession) of 41263 river reaches globally on yearly and multiyear scales.~~of 5548 river reaches globally .~~ Streamflow i~~The i~~ndices values until 2022 are ~~time series~~covered in the dataset ~~are available until 2021~~. Time span of the time series dataset is from 1806 to 2022 with an average length of 36 years.~~, the lengths of which vary from 30 to 215 years with an average of around 66 years. Restricted-access streamflow data of typical river basins in China are included in the dataset.~~ Compared to existing global datasets, this global dataset covers more stations and more indices, especially those characterizing the frequency, duration, changing rate, and recession of streamflow regime. ~~,~~ With the dataset, research on streamflow regime will become easier without spending time handling raw streamflow records. This comprehensive dataset will be a valuable resource to the hydrology community to facilitate a wide range of studies, such as studies of hydrological behaviour of a catchment, streamflow regime prediction in data-scarce regions, as well as variations in streamflow regime from a global perspective.

The dataset can be accessed at https://doi.org/10.57760/sciencedb.07227.

1 Introduction

Streamflow regime plays a vital role not only in human life and activities but also in the native biodiversity, ecosystem integrity, and biogeochemical cycles (Poff et al., 1997; Paine, 2019; Palmer and Ruhi, 2019). Because of the effects of anthropogenic activities and climate change especially in the last decades, streamflow regimes of many rivers worldwide have been changing, threatening the water security (Torabi Haghighi et al., 2021; Tonkin et al., 2018; Chen et al., 2023b; Chen et al., 2021). A large number of studies have been done to reveal the streamflow regime shifts, their causes and consequences (Worku et al., 2014; Brouziyne et al., 2021; Sauquet et al., 2021; Lane and Kay, 2021; Yin et al., 2018). Palmer and Ruhi (2019) found that the dam ~~building~~construction, diversion or abstraction of water, clearing of land, and climate change increasingly degraded the river ecosystems by altering their streamflow regimes. Barichivich et al. (2018) indicated that the streamflow regime shifts over the Amazon basin in magnitude and frequency, which has caused major human suffering and disturbance to the rainforest ecosystems, are driven by strengthened Walker circulation.

In order to analyse the streamflow regime shifts, the critical components of the streamflow regime, *i.e.*, magnitude, frequency, duration, timing, and rate of change, were proposed to characterize the entire range of streamflow regime and specific hydrologic phenomena (Poff and Ward, 1989; Poff et al., 1997; Richter et al., 1996). By using indices of these components, features of streamflow regime can be considered explicitly, and therefore ~~these~~indices of components have been~~are~~ widely used (Olden and Poff, 2003; Worku et al., 2014; Palmer and Ruhi, 2019; Shih et al., 2022; Jacobson et al., 2022; Harmon et al., 2022; Wasko et al., 2020). ~~Besides, inspired by this~~In past decades, more and more indices~~, signatures,~~ and components have been~~are~~ proposed to represent different aspects of streamflow regime (Clausen and Biggs, 2000; Baker et al., 2004; Clark et al., 2009; Botter et al., 2013; Mcmillan et al., 2017; Gnann et al., 2021a). ~~For example, Baker et al. (2004) presented a new flashiness index based on daily streamflow to characterize the flashiness of streamflow regime, which was later widely used (Gnann et al., 2021b).~~ However, except for several basic indices of magnitude and frequency like the annual maximum streamflow (Do et al., 2017; Barichivich et al., 2018), there are few large-sample and global studies on other components such as timing, variability, and rate of change. Gudmundsson et al. (2018) found that there was no any study analysing time series of the variability (e.g., standard deviation, coefficient of variation, Gini coefficient, and the inter quartile range) and timing (e.g., the timing of annual minimum flow, day of minimum 7-day mean streamflow, and day of maximum 7-day mean streamflow) of daily streamflow on a global scale.

Large-sample hydrology is a way to go beyond individual case studies and to draw robust conclusions on hydrological processes from a big-picture perspective (Gupta et al., 2014; Addor et al., 2020). Currently, due to the increasing availability of large-sample hydrology datasets, as well as the booming big data techniques, more and more large-sample hydrological studies have been appearing, significantly advancing the hydrology science (Sun et al., 2021; Troin et al., 2022; Lane et al., 2022; Goeking and Tarboton, 2022; Nearing et al., 2021; Gnann et al., 2021a; Gudmundsson et al., 2021). To perform large-sample hydrological analysis, large-sample hydrological datasets based on gauged ~~flow~~ recordsdata are mostly needed. Addor et al. (2017) presented the CAMELS (Catchment Attributes and MEteorology for Large-sample Studies) dataset, which synthesized various datasets (including meteorological forcing and gauged daily streamflow time series) to describe attributes of catchments and catchment behaviours in the contiguous United States. Afterwards, diverse versions of CAMELS or CAMELS-like datasets were presented for different countries, such as the Great Britain (Coxon et al., 2020), Chile (Alvarez-Garreton et al., 2018), Brazil (Chagas et al., 2020), Australia (Fowler et al., 2021), Central Europe (Klingler et al., 2021), France (Delaigue et al., 2022), and Germany (Ebeling et al., 2022). Indices datasets of streamflow regime have also been developed on both ~~Besides, there are also~~ regional (like ADHI by Tramblay et al. (2021)) scale and global scale (like GSIM by Do et al. (2018) and Gudmundsson et al. (2018))~~(Do et al., 2018; Gudmundsson et al., 2018)streamflow indices datasets (Tramblay et al., 2021) and global streamflow indices and metadata archive (GSIM) for analyses on regional and global streamflow characteristics (Do et al., 2018; Gudmundsson et al., 2018). Unfortunately, many original records of gauged streamflow are not open access, and are forbidden to be shared due to certain policies. In contrast, the data products derived from restricted access streamflow records are usually allowed to be shared. Thus, streamflow indices datasets not only facilitate the research on streamflow regimes, but also are good alternatives when the original records of streamflow are hard to access (Tramblay et al., 2021; Mcmillan et al., 2017)~~.

GSIM covers time-series indices of more than 30000 stations worldwide, which represents the water balance, the seasonal cycle, low flows, and floods, with the latest streamflow indices values~~data~~ until 2016~~7~~. It is ~~without doubt~~ one of the most popular datasets which facilitate large-sample research on global streamflow. However, GSIM only includes the streamflow regime components that characterize the magnitude, timing, and variability without ~~, but does not~~ includinge components characterizing the frequency, duration, changing rate, and recession of streamflow regime. In fact, these components are very useful for~~to~~ fully characterizinge the streamflow~~flow~~ regime, understanding its functions, and ~~analy~~analysing~~se~~ its variations. T~~For instance,~~he frequency and duration of streamflow regime are crucial to studies on various flow events~~the frequency and~~

~~duration of streamflow regime are very important in describing various flow events~~. Gehrke et al. (1995) discovered~~found~~ that in the Murray-Darling river system, the altered frequencies of high and low flow events have a significant impact on the species diversity of fish communities. Colls et al. (2019) ~~analysed~~ examined the frequency and duration of zero flow events over 33 Mediterranean streams ~~in NE Iberian Peninsula~~ and found~~indicted~~ that longer duration of zero flow events significantly decreases gross primary production by promoting heterotrophy. Changing rate is an important factor affecting the lives of aquatic species. For example, rapid changes of river stage caused by hydroelectric facilities will damage downstream aquatic species by wash-out and stranding (Cushman, 1985). Besides, the increase of changing rate during storms will result in elevated concentrations of pollutants, which is harmful to the lives of aquatic species~~ reviewed the changing rate of streamflow regime below hydroelectric facilities and found that the rapid changes of river stage has damaged aquatic species by wash-out and stranding.~~ (Palmer and Ruhi, 2019). ~~added that the increase of changing rate during storms results in elevated concentrations of pollutants, which is also harmful to the lives of aquatic species.~~ The recession of streamflow reflects the low-flow behaviour of a catchment and plays a vital role in both flow-biota-ecosystem processes nexus and water management. For instance, ~~Boggaart et al. (2016) used streamflow recession patterns to unravel the role of climate and humans in landscape co-evolution.~~ Rood et al. (1995) ~~did a study on the recession of streamflow and present~~indicated that the accelerated flood recession had resulted in the failure of seedling establishment and the decline of riparian cottonwoods along the St. Mary River. The importance of analysing flood recession has also been emphasized to mitigate flood risks and optimize water utilization in the Huaihe River Basin (Cheng et al., 2021) ~~indicated that analysis on recession of flood is critical for flood risk reduction and water use in the Huaihe River Basin~~. In this regard, a more comprehensive indices dataset than GSIM is needed. Actually, Tramblay et al. (2021) presented the African Database of Hydrometric Indices (ADHI, 1950–2018) with a more comprehensive streamflow indices, but it is geographically limited to the Africa. There is a lack of a~~no~~ comprehensive global large-sample dataset of~~of different~~ component~~s~~ of streamflow regime, which hinders research on streamflow regime, especially on a global scale.

In this paper, we collected and merged daily streamflow records from 9 data sources into one collection, and then performed a data quality control on the collection. After that, a new global streamflow indices time series dataset was developed. The spatiotemporal coverage, quality, metadata, and sample values of the dataset are also shown in the following sections.~~augmented the gauged daily streamflow data from Global Runoff Data Centre (GRDC) by collecting streamflow data from India Water Resources Information System (WRIS), Arctic Great Rivers Observatory (ArcticGRO), and China Hydrological Yearbooks (CHY) to build a daily streamflow data collection. After that, quality control was done to guarantee reasonable values as well as a longer record length. Next, indices spanning 7 components of streamflow regime, *i.e.*, magnitude, frequency, duration, changing rate, timing, variability, and recession, were defined and calculated to build a new global streamflow indices dataset. Finally, an exemplary analysis on the temporal concentration of streamflow on a global scale was presented to illustrate the use of the dataset.~~

2 Data compilation~~Data sources and processing~~

~~1.1~~2.1 Data collection~~collecting~~

The daily streamflow records used for the establishment of a global streamflow indices time series dataset were collected from 9 data sources, *i.e.*, Global River Discharge Centre (GRDC), U.S. Geological Survey (USGS) National Water Information System, National Water Data Archive of Canada (HYDAT), National Water Agency of Brazil (ANA), the Chilean Centre for Climate and Resilience Research (CCCRR), Arctic Great Rivers Observatory (ArcticGRO), China Hydrological Yearbooks (CHY), India Water Resources Information System (WRIS), and Australia Water Data from Australian Bureau of Meteorology (BOM) (see Table 1 for details). ~~data of the daily streamflow data collection are from Global Runoff Data Centre (GRDC) at~~

https://www.bafg.de/GRDC/EN/02_srvcs/21_tmsrs/riverdischarge_node.html and other three sources, i.e., India Water Resources Information System (WRIS) at https://indiawris.gov.in/wris/#/, Arctic Great Rivers Observatory (ArcticGRO) at https://arcticgreatrivers.org/, and China Hydrological Yearbooks (CHY). These data sources are all publicly available except the CHY. The original records of streamflow in CHY are restricted-access and hard to collect, and thus only some streamflow data of some typical river basins were were collected including . 30 stations in 7 largest river basins in China. Among these data sources, USGS, HYDAT, ArcticGRO, and BOM provide quality flags of records. The total amount of hydrological stations in the data collection is 15408

, the summary of these stations is shown in Fig. 1. GRDC and ArcticGRO are international datasets having multiple countries' records, and some records may overlap with records from other national datasets. The duplicated data can to some extent interfere with users' utilization of the data. We calculated the distances between each station in the international datasets and each station in the national datasets. When this distance was less than 60m (approximately 0.0005 degrees on the equator), these two stations were considered the potential identical station. After that, a further inspection was performed to verify whether these two stations were the same station according to the name of river and station. A total of 1895 duplicated stations were found including 8 stations in ArcticGRO, 321 stations in ANA, 324 stations in BOM, 68 stations in CCCRR, 2 stations in CHY, 439 stations in HYDAT, and 733 stations in USGS. We retained stations with longer record length and removed duplicate stations with shorter record length. A total of 41263 stations were retained and then merged into a streamflow records collection.

Apart from the streamflow records, there are metadata of each station in every data source. However, the fields of metadata vary among different data sources. Some metadata have many fields while the others only have basic fields. For the purpose of standardization, fields of metadata of our collection include station ID, data source, river name, station number, country, latitude, longitude, contributing area, altitude, start year, end year, years, days, and missing ratio.

The Americas and Europe witness extensive streamflow records with high spatial coverage density and long record length (Figure 1a). In contrast, there are relatively few records in Asia and Africa. Around 20000 stations (50%) have streamflow records with lengths more than 30 years (Figure 1b), and more than 2000 stations' (5%) record lengths are larger than 100 years. The stations with a more than 100 years record length are mainly It should be noted that 9171 stations have daily streamflow records, while the others only have basic information of stations without daily streamflow records. The daily streamflow record lengths vary from 1 to 215 years.

The GRDC is very comprehensive in terms of the record length and spatial coverage of gauged daily streamflow data. The spatial density and record lengths of streamflow time series in the Americas, Europe, Southern Africa, Western Africa, and Oceania are high and long (Fig.1a). There are 10711 hydrological stations in GRDC, out of which 8552 stations have daily streamflow records. The daily streamflow records range from 1806 to 2021 and the lengths vary between 1 and 215 years. However, although there are enormous stations in Asia included in GRDC, almost all of their record lengths are shorter than 10 years, which largely reduces their value for hydrological analyses. Therefore, we combined GRDC with ArcticGRO, CHY, and WRIS to build an augmented data collection. India-WRIS provides water resources data and information of watersheds in India for planning, development, and integrated water resources management. It includes 4648 stations, but only 570 stations have daily streamflow records. The daily streamflow records ranging from 1960 to 2021 are used to build the data collection. ArcticGRO provides essential data about the biogeochemistry and discharge of the largest Arctic rivers. It covers 16 stations with daily streamflow records ranging from 1927 to 2021 and the record lengths vary from 5 to 95 years. 33 stations from CHY with daily streamflow records ranging from 1947 to 2020 are used to build the data collection. The record lengths vary from 1 to 73 years. These stations are of typical river basins and located in 7 largest river basins in China, *i.e.*, Yangtze River

~~Basin, Yellow River Basin, Huai River Basin, Haihe River Basin, Songhua River Basin, Liao River Basin, and Pearl River Basin.~~

~~In our streamflow data collection, streamflow record lengths at more than 700 stations are more than 100 years, most of which are distributed~~ in ~~the United States~~North America and Europe. ~~About 6000 stations (67%) are of lengths between 30-100 years, while the others (33%) are of lengths less than 30 years (Fig.1b).~~ As for the ~~temporal distribution of numbers~~availability of ~~stations with gauged daily streamflow data~~streamflow records in different years, the number of stations with available records increases from 1900 to 197~~887~~ at a peak of around 18000~~7500~~, and then keeps fluctuating but relatively stable from 1979 to 2015, followed by a decrease from 2016 to 2022 at a bottom of 12000 (Figure 1c). Overall, the streamflow records collection has 41263 stations with an average record length of 36 years. The time span of the collections is from 1806 to 2022.

~~and it drops from 1987 to 2021 at a bottom of nearly 1400 (Fig.1c).~~

Table 1. Summary of nine measured streamflow data sources

Database	Spatial coverage	Time span	Included catchments	Data access	Quality f~~F~~lag
Global River Discharge Centre (GRDC)	Globe	1806-2022	8458	https://www.bafg.de/GRDC/EN/Home/homepage_node.html	-
U.S. Geological Survey (USGS) National Water Information System	US and Canada	1857-2022	19269	https://waterdata.usgs.gov/nwis?	A: value has been validated to be published A:e: value was estimated and validated to be published P and P:e: Provisional data
National Water Data Archive (HYDAT)	Canada	1860-2022	5786	https://www.canada.ca/en/environment-climate-change/services/water-overview/quantity/monitoring/survey/data-products-services/national-archive-hydat.html	A: Partial Day (numeric value 1) B: Ice Conditions (numeric value 2) D: Dry (numeric value 3) E: Estimated (numeric

Database	Spatial coverage	Time span	Included catchments	Data access	Quality flag
					value 4) S: Sample(s) collected this day (numeric value 5)
National Water Agency (ANA)	Brazil	1901-2022	3691	https://www.ufrgs.br/lsh/products/ana-data-acquisition/	-
the Chilean Center for Climate and Resilience Research (CCCRR)	Chile	1913-2018	767	https://www.cr2.cl/datos-de-caudales/	-
Arctic Great Rivers Observatory (ArcticGRO)	The largest Arctic rivers	1927-2022	17	https://arcticgreatrivers.org/	A: certified data P: provisional data
China Hydrological Yearbooks (CHY)	China	1947-2020	30	No public access	-
India Water Resources Information System (WRIS)	India	1960-2021	161	https://indiawris.gov.in/wris/#/	-
Australia Water Data Online, Australian Bureau of Meteorology (BOM)	Australia	1881-2022	4977	http://www.bom.gov.au/waterdata/	A (flag 10): best available B (flag 90): compromised to represent the parameter C (flag 110): estimated value E (flag 140):

Database	Spatial coverage	Time span	Included catchments	Data access	Quality fFlag
					quality is not known F (flag 210): poor quality or missing Flag “-1” also presents to indicate missing value

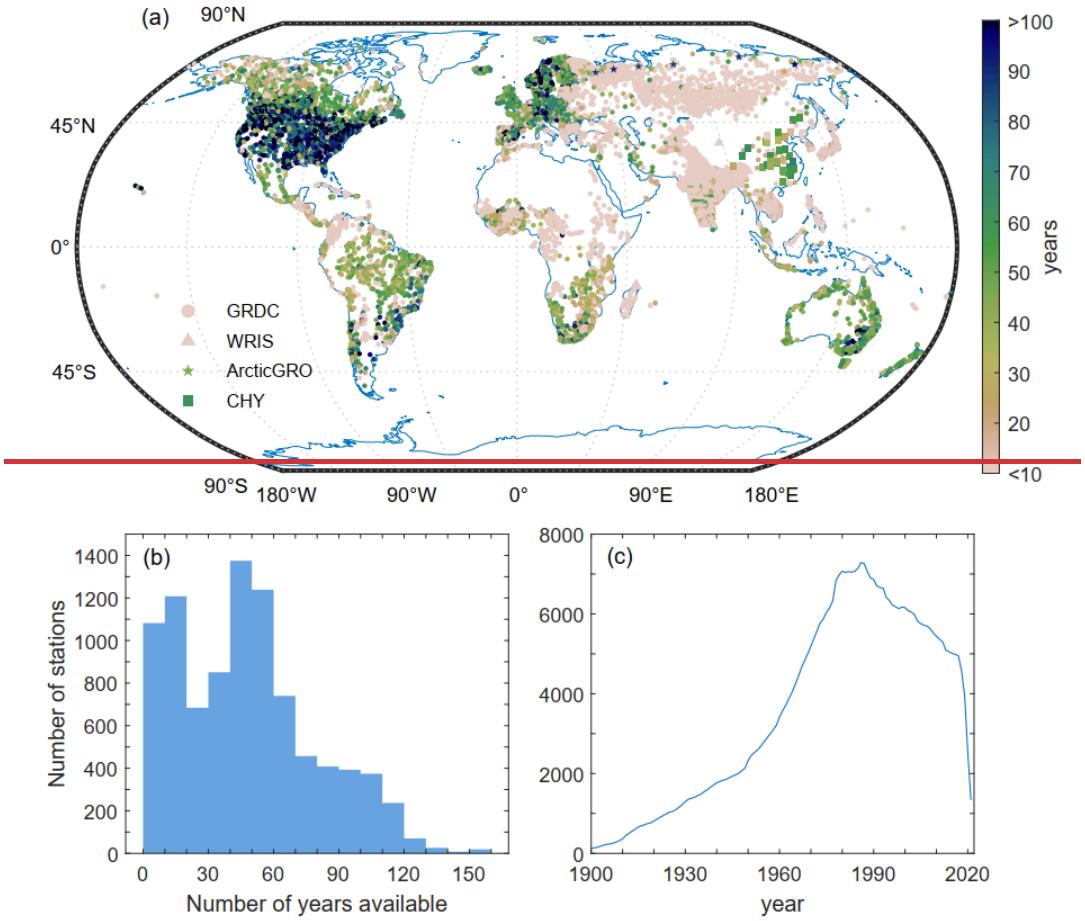
(a)
90°N
45°N
0°
45°S
90°S
180°W
90°W
0°
90°E
180°E
GRDC
WRIS
ArcticGRO
CHY
>100
90
80
70
60
50
40
30
20
<10
years

(b)
Number of stations
Number of years available
(c)
year

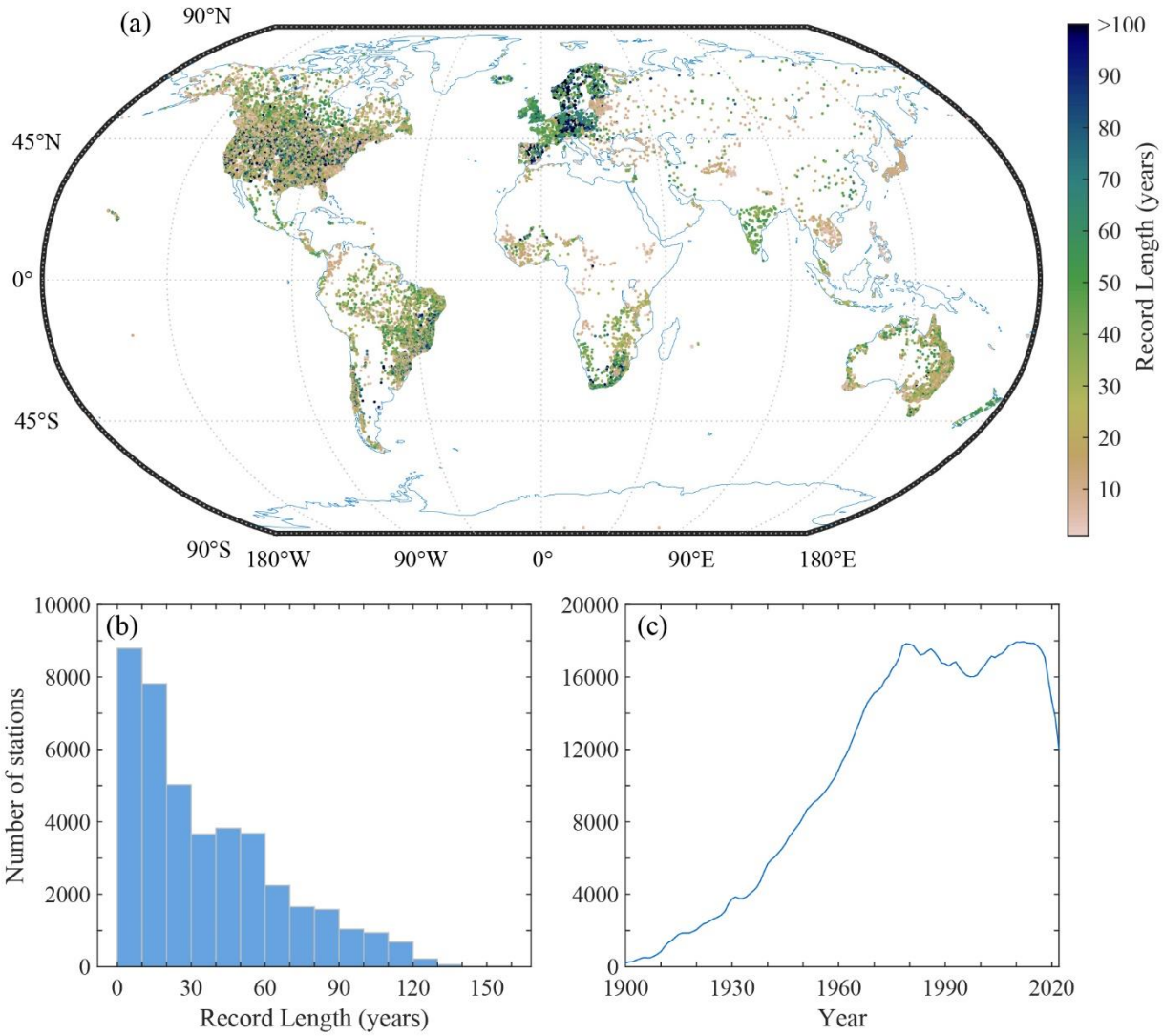

Figure 1. A summary of the streamflow records ~~data~~ collection. (a) shows the spatial distribution and~~,~~ record lengths~~, and sources~~ of daily ~~flow~~ streamflow records~~time series~~. (b) illustrates number of stations with ~~available for~~ different record ~~record~~ lengths~~, and stations without gauged streamflow data are not included~~. (c) shows number of stations with records in every year~~with gauged streamflow data available every year~~ from 1900 to 2021~~1~~. Refer to https://doi.org/10.57760/sciencedb.07227 for vector graphic that shows all the stations clearly without overlap since the vector graphic can be zoomed in infinitely without losing any detail.

2.2 Data quality

2.2.1 Quality flag of records

Data quality control is necessary before the use of data as poor-quality data are misleading. Some data providers have inspected the data before publication and attached data quality flags to the published data, while the others have not. Data quality flags represents data quality and thus are important to quality control. The flags vary among different data providers (Table 1). For the purpose of standardization, the original flags were translated into four flags in our streamflow records collection, *i.e.*, *reliable*, *suspect*, *no flag*, and *missing* (see Table 2 for the rules). As for the databases without quality flags, available records were flagged as *no flag* while missing records were flagged as *missing*. ~~Data quality control~~

For records with poor-quality flag or no flag, some ~~scholars~~studies, like Gudmundsson et al. (2018), performed automatic detection methods to identify and remove unreasonable streamflow values, including consecutive equal values and outliers. However, the criteria for judging whether data is unreasonable primarily rely on subjective assumptions. To the best of our knowledge, the applicability and possible impacts of such criteria have not been assessed yet. It is still disputable whether and how many correct values are erroneously flagged as incorrect and removed (Crochemore et al., 2020; Tramblay et al., 2021).

The mistakes will diminish the utility of the data. For example, some extreme flood events may be flagged as outliers and removed, resulting in an underestimation of flood. Therefore, we did not perform disputable automatic detection methods. A reliable automatic detection method was applied as follows.

Considering possible mistakes made by instruments and humans, negative daily streamflow values may occur in the streamflow records collection, which are undoubtedly wrong values. If a daily streamflow value is a negative number, this value will be removed and flagged as *missing*. Besides, if quality flags are initially absent in time series where there are negative values, the whole time series will be flagged as *suspect*. A total of 40842 negative streamflow values were detected and removed.

In addition to each record, quality flags were also attached to each station according to the criteria in Table 3. There are 235 million records (43%) showing *reliable*, 221 million records (41%) showing *no flag*, 6.9 million records (1%) showing *suspect*, and 79 million records (15%) showing *missing* (Figure 2a). Numbers of stations with flags A, B, C, D, E are 6952 (17%), 7094 (17%), 8772 (21%), 6571 (16%), and 11874 (29%) respectively (Figure 2b). Quality flags of records were used to assess the quality of indices that were calculated based on the records in the following text. Quality flags of stations were designed to allow users to pick appropriate stations whose records' quality meets users' quality control requirements.

Table 2. Translation of quality control flags of the original databases to flags of the streamflow records collection.

Data Source	Original Quality Flag	*Reliable*	*Suspect*	*No Flag*	*Missing*
USGS	A: validated data A:e: estimated and validated data P and P:e: Provisional data	A, A:e	P, P:e		
HYDAT	A: Partial Day B: Ice Conditions D: Dry E: Estimated S: Sample(s) collected this day	B, D, S	A, E		
ArcticGRO	A: certified data P: provisional data	A	P		
BOM	A: best available B: compromised to represent the parameter C: estimated value E: quality is not known F: poor quality or missing -1: missing value	A, B	C	E	F, -1

Table 3. Criteria for quality control flags of stations. Note that when one station's records meet multiple criteria simultaneously, the highest-level flag is applied.

Flag	Criterion
A (or numeric value 1)	More than 95% of record flags are *reliable*
B (or numeric value 2)	More than 95% of record flags are *reliable* or *no flag*
C (or numeric value 3)	Less than 10% of record flags are *missing*
D (or numeric value 4)	Less than 20% of record flags are *missing*

E (or numeric value 5)	At least 20% of record flags are *missing*

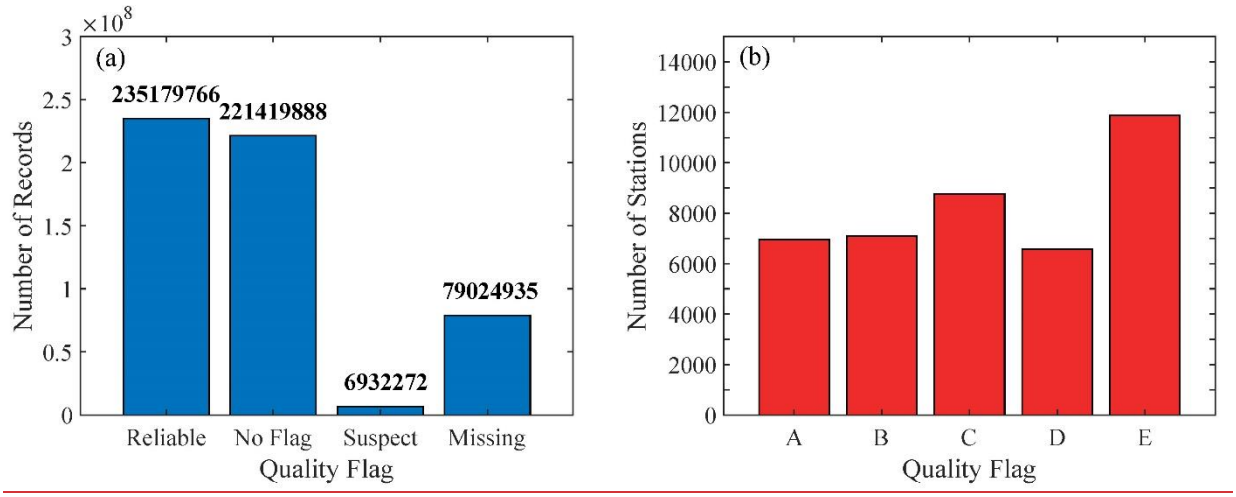

Figure 2. Numbers of (a) records and (b) stations with each quality flag.

2.2.2 Temporal coverage and missing ratio

In the streamflow records collection, ~~In order to build a high-quality, long-time-series, and reliable global streamflow indices dataset, data quality control on the data collection is needed before further calculations. An Automatic detection method was applied to identify the suspect observations according to three quality control criteria detailed below, and modifications were done to the suspect observations:~~

~~1. Considering possible mistakes made by instruments and humans, negative daily streamflow values may occur in the data collection, which is non-physical and must be revised. If a daily streamflow value is a negative number, this value will be regarded as a suspect value, and then this value will be changed into an average value of the two adjacent values. A negative value detected in the time series of Jenapur at Brahmani, India from WRIS is shown for the purpose of illustration (Fig.2a).~~

~~If there are more than 10 consecutive equal values bigger than 0 and 50th percentile of daily streamflow in corresponding year, they will be regarded as suspect values, and then they will be changed into missing values. There are many reasons for the consecutive equal values. It may occur because of instrument failure, *i.e.*, damaged sensors and ice jams, or flow regulations (Gudmundsson et al., 2018). Moreover, it also happens when the day-to-day fluctuations of streamflow are below the sensitivity of the employed sensor (Gudmundsson and Seneviratne, 2016). Because this issue usually occurs during the low flow period, we choose the 50th percentile of daily streamflow as the threshold to exclude those abnormal cases. The selection of 10 days is according to Gudmundsson et al. (2018). Consecutive equal values found in the time series of Etemba at Omaruru, Namibia from GRDC are shown for the purpose of illustration (Fig.2b).~~

~~2. According to Gudmundsson et al. (2018), if $\log(Q+0.01)$ is bigger or smaller than the mean value of $\log(Q+0.01)$ plus or minus 6 times the standard deviation of $\log(Q+0.01)$, where Q is a daily streamflow value and the mean value and standard deviation are calculated in a 5-day window centred on the calendar day of Q, the Q will be regarded as an outlier and changed into an average value of the two adjacent values. Following Gudmundsson et al. (2018), the 6 standard deviation threshold is reasonable, because it keeps a balance between screening out outliers that could come from instrument malfunction and retaining the extreme floods or low flows. An outlier detected in the time series of Luanxian at Luanhe River, China from CHY is presented for the purpose of illustration (Fig.2c).~~

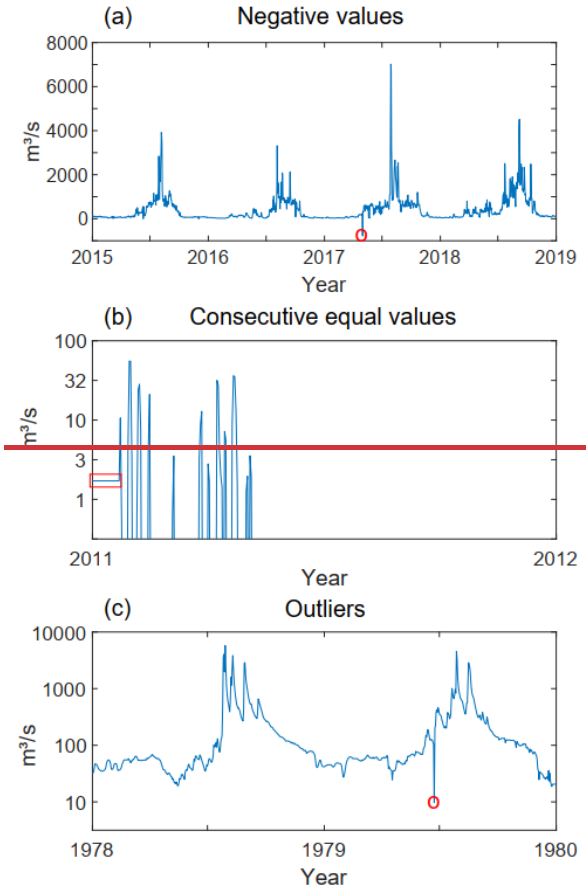

~~**Figure 2. Three example time series illustrating issues detected by the three quality control criteria (highlighted in red). (a) shows the negative value detected in the time series of Jenapur at Brahmani, India from WRIS. (b) presents the consecutive equal values found in the time series of Etemba (64733002) at Omaruru, Namibia from GRDC. (c) illustrates one outlier in the time series of Luanxian at Luanhe River, China from CHY. The common logarithmic axis is used in (b) and (c).**~~

~~After automatic detection and modification of suspect observations, a final data quality control is applied. That is, the time series with the date of latest records before 2000 or lengths shorter than 30 years were removed, since they are outdated and less convincing for streamflow regime analyses. In the end, 5548 time series were remained for the calculation of indices.~~

~~The availability of daily streamflow data after data quality control is shown in Fig.3.~~ more than 6000~~Nearly 1500~~ stations have a record length of ~~72~~ 32 years from ~~1950~~ 1990 to 202~~1~~ with missing ratios less than 5%, and around 800 stations have a record length of 102 years from 1920 to 2022 with missing ratios less than 5% (Figure 3a). As for year of the latest record, approximate 12000 stations' records end in 2022, while around 17000 stations' records are absent after 2000 (Figure 3b). ~~only 5% missing data, and around 3000 stations have a record length of 52 years from 1970 to 2021 with 10% missing data (Fig.3a). At approximate 800 stations, their streamflow records are not available since 2013 (Fig.3b). By comparison, at more than 4000 stations, streamflow records are available even after 2017. At around 2400 stations, the latest streamflow records are available till 2020 or 2021.~~

Fig~~.~~ure 3c shows the number of stations for every year from 1900 to 2022 with different missing ratios of records ~~the number of stations available every year from 1900 to 2021 with various missing data rates~~. All curves ~~in Fig.3c~~ show similar trends. The number of stations gradually rises from 1900 to its peak in~~at~~ around 197~~885~~, and then keeps fluctuating but relatively stable from 1979 to 2013, followed by a decrease from 2014 to 2022. More than 80% of stations with records have no missing records for every year from 1900 to 2022 (Figure 3c). Furthermore, more than 50% of stations have a record length of more than 30 years and have no missing records for every year from 1900 to 2022. There are around 15000 stations having no missing records for every year from 1975 to 2018.

~~and then it keeps slightly dropping until around 2010, followed by a drastic decrease until 2021. With regard to the missing data rate, the stations numbers are around 4500 with missing data rate < 1% and around 4700 with missing data rate < 5% in 1980-2005. In 2020, there are still around 1200 stations available with missing data rate < 1%.~~

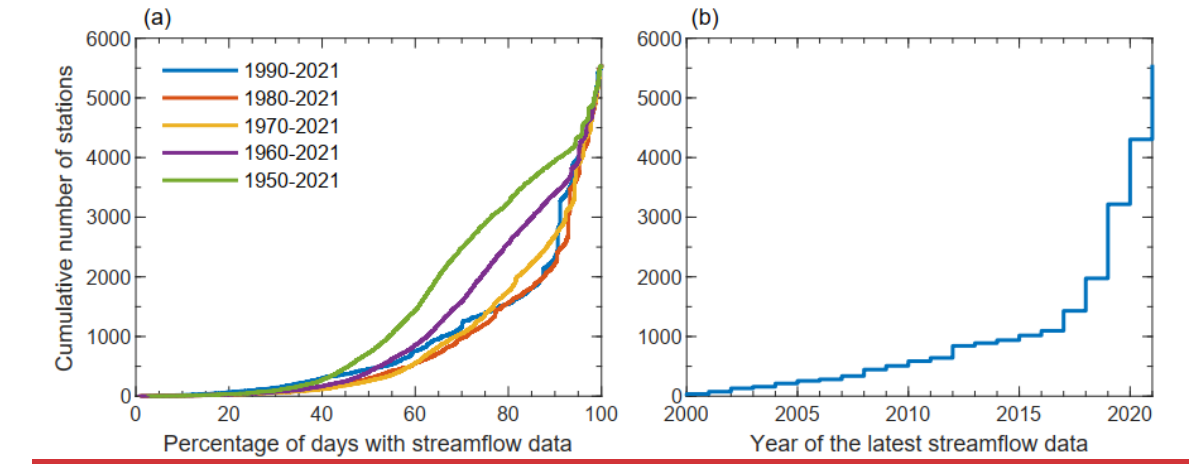
(a)
(b)
Cumulative number of stations
1990-2021
1980-2021
1970-2021
1960-2021
1950-2021
Percentage of days with streamflow data
Year of the latest streamflow data

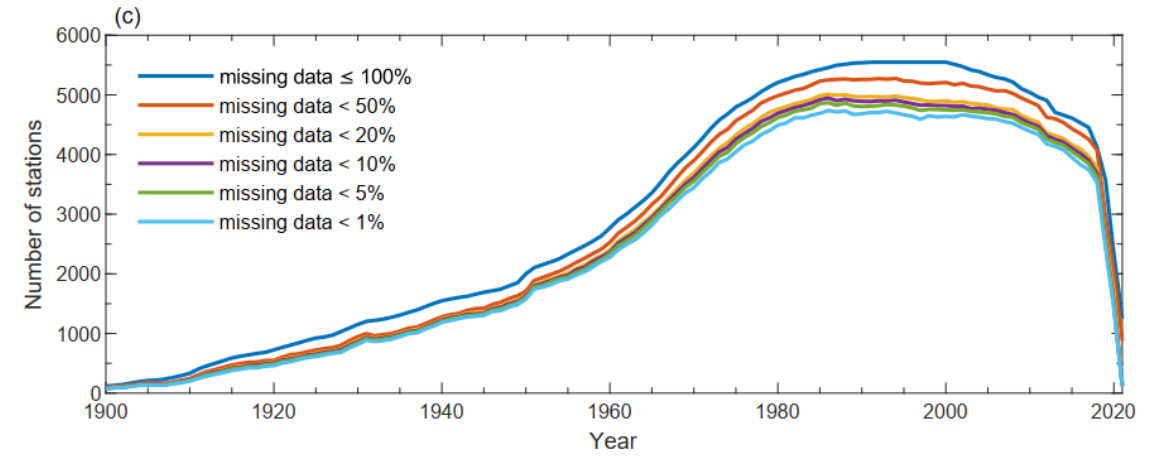
(c)
Number of stations
missing data ≤ 100%
missing data < 50%
missing data < 20%
missing data < 10%
missing data < 5%
missing data < 1%
Year

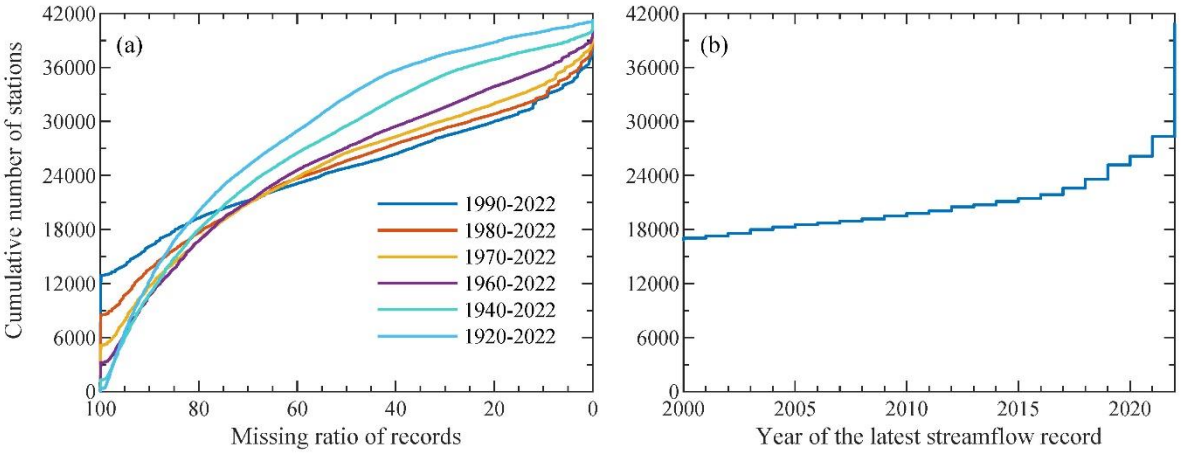
(a)
(b)
Cumulative number of stations
1990-2022
1980-2022
1970-2022
1960-2022
1940-2022
1920-2022
Missing ratio of records
Year of the latest streamflow record

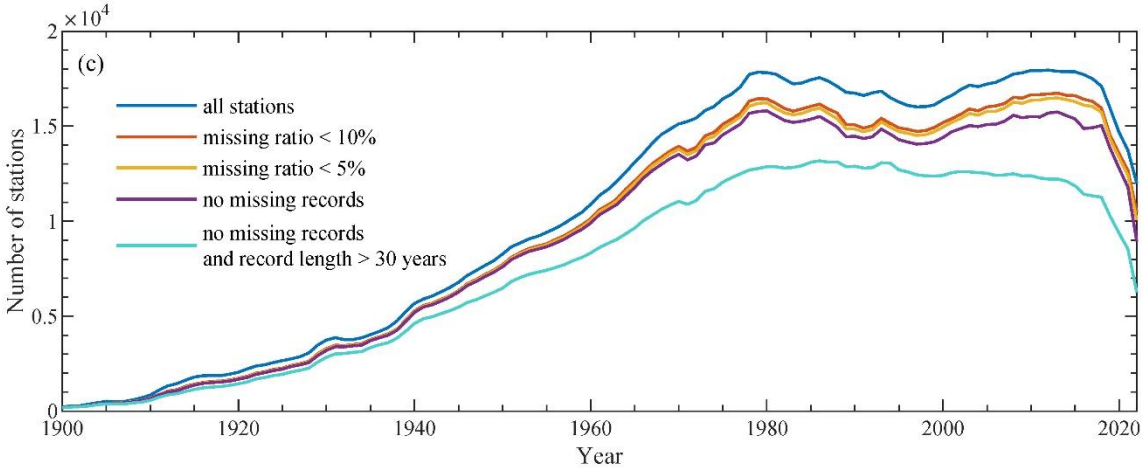
(c)
Number of stations
all stations
missing ratio < 10%
missing ratio < 5%
no missing records
no missing records
and record length > 30 years
Year

Figure 3. Temporal coverage and missing ratio of streamflow records. ~~Availability of daily streamflow data after data quality control.~~ **(a)** shows the cumulative number of stations corresponding to different missing ratios of records in different time spans. (b) shows the cumulative number of stations corresponding to different years of the latest streamflow record. (c) ~~and (b) show the cumulative distribution of stations corresponding percentage of days with streamflow data in different record lengths and year of the latest streamflow data, respectively. (c)~~ presents number of stations foravailable every year from 1900 to 2021 with differentvarious missing ratios of recordsdata rates.

3 Streamflow indices

~~1.2~~3.1 Indices definition and calculation ~~and calculation~~

Table ~~4~~1 describes 79 streamflow ~~time series~~ indices that characterize seven components of streamflow regime, *i.e.*, magnitude, frequency, duration, changing rate, timing, variability, and recession on yearly and multi-year scales. These indices were ~~calculated~~calculated based on ~~from~~ the streamflow records ~~data~~ collection ~~after the data quality control~~, and ~~, and m~~most of them were~~are~~ computed with the Toolbox for Streamflow Signatures in Hydrology (TOSSH, available at the address: https://github.com/TOSSHtoolbox/TOSSH) (Gnann et al., 2021b). ~~Only data in years with less than 5% missing data are included in indices calculation.~~

The magnitude of streamflow regime ~~can~~ reflects the amount of streamflow from various perspectives. ~~The c~~Corresponding indices include: (i) maximums of consecutive 1, 3, 7, and 30 day streamflow averages and their percentages, which indicate the magnitude and concentration of high flows and floods; (ii) minimums of consecutive 1, 7, and 30 day streamflow averages, which indicate the magnitude of low flows; (iii) various percentiles of streamflow; (iv) monthly and ~~/~~annual mean flow, which are~~is~~ usually used for water resources analysis; (v) high and ~~/~~low flow event threshold (Clausen and Biggs, 2000; Olden and Poff, 2003); (vi) runoff and ~~/~~baseflow magnitude (Horner, 2020), which indicate~~s~~ the magnitude of difference between the maximum and the minimum of runoff and ~~/~~baseflow.

The frequency of streamflow regime is how often a flow of specific magnitude recurs over some specified time intervals (Poff et al., 1997). The corresponding indices include the ratios of days with streamflow reaching specific thresholds to the total days and the numbers of streamflow events (floods, high flows, low flows and so on) with various thresholds. The duration is the period of time during which a streamflow event lasts. Annual mean durations of streamflow events are calculated as indices.

The changing rate, or flashiness, means how fast and frequently streamflow alters from one magnitude to another (Poff et al., 1997; Baker et al., 2004). A flashy river basin has a very quick and sensitive response to incoming water like precipitation with rapidly rising and falling hydrographs~~, and its streamflow rises and falls very rapidly~~. The Richards-Baker flashiness index (Baker et al., 2004), and the mean and median of all positive/negative differences between consecutive daily streamflow values (The Nature Conservancy, 2009) are used to quantify the flashiness of streamflow. Rising limb density is an index that describes the flashiness of the catchment response; for example, a small value means a smooth hydrograph (Sawicz et al., 2011).

The timing of streamflow regime is the temporal distribution of streamflow in a year (Court, 1962), which is charactered by the start date of flood season, half flow date, half flow interval, momentary maximum date, and minimum consecutive 7 day flow date in the indices dataset. To calculate the half flow date and half flow interval, the start of the water year is needed (Court, 1962). Although it is widely used that the start of the water year is 1 October in the Northern Hemisphere and 1 July in the Southern Hemisphere, the actual starts of the water year vary greatly even in different river basins of one hemisphere because of different geographical features, climates and so on. In the indices dataset, we use the start date of flood season as the start of the water year. The start date of the flood season for a specific station is the median of start dates of consecutive 180 days, ~~-~~of which the streamflow average is the biggest ~~-~~in one calendar year.

The indices of variability characterize the variability of streamflow regime from different perspectives (Gudmundsson et al., 2018). (i) Variance of streamflow time series provides information on the total variability of streamflow. (ii) Coefficient of variation of streamflow provides a relative measure of variability that is independent of the mean flow. (iii) Quartile-based coefficient of variation of streamflow time series provides information about the width of the distribution centre and is less sensitive to outliers. (iv) Ratio of the maximum to median of streamflow quantifies the deviation of maximum. (v) The Gini coefficient is an index to measure the inequality among values of flow duration curve ~~(Gudmundsson et al., 2018)~~. (vi) Slope of flow duration curve is an index of the variability of the seasonal water balance, which shows the difference between high and low flows (Mcmillan et al., 2017). Besides, it is also sensitive to vertical redistribution of soil water between quick flow and slow flow. (vii) Slope of distribution of peaks is an index for measuring the differences between peak discharges (Euser et al., 2013). (viii) Variability index was a measure for variability among values of flow duration curve (Lane and Lei, 1950). A river with higher variability index tend to have higher percentage of surface runoff and lower water storage (Estrany et al., 2010).

Recession is a component of streamflow regime which characterizes the recession of streamflow. The smoothed minima baseflow separation method of the UK Institute of Hydrology (UKIH) (1980) is used for baseflow separation required in the calculation of recession indices. Recession indices include baseflow index and baseflow recession constant. Generally, a river with low baseflow index value has a great number of floods and low flows, and its streamflow regime is highly variable (Singh et al., 2019). Baseflow index has been commonly used in regional low flow studies, impacts of climate change on groundwater resources, and flood responses of river basins to storm events. Baseflow recession constant is a proxy for drainage efficiency of baseflow after being recharged, which is related to the watershed hydraulic conductivity, soil porosity, and hydraulic gradient (Safeeq et al., 2013). According to Safeeq et al. (2013), a river basin with high baseflow recession constant has a shallow subsurface flow-dominated fast draining system, whereas a river basin with low baseflow recession constant has a groundwater-dominated slow draining system.

Table ~~4~~1. Streamflow indices for seven components of the streamflow regime. Index name means the variable name used in the indices time series dataset. There are two temporal resolutions. Y (yearly) means one value for one year of the time series, and MY (multi-year) means one value for the whole time series.

Category	Index name	Units	Resolution	Definition
Magnitude	*Qmax1, Qmax3, Qmax7, Qmax30*	m^3/s	Y, MY	Maximums of consecutive 1, 3, 7, and 30 day~~s~~ streamflow averages. For example, *Qmax7* means the maximum of consecutive 7-day streamflow averages (Olden and Poff, 2003).
	Qmax1p, Qmax3p, Qmax7p, Qmax30p	-	Y	~~The~~ percentages of the maximum~~s~~ of consecutive 1, 3, 7, and 30 day~~s~~ streamflow accumulation amounts, which are the maximum~~ss~~ divided by the ~~total of~~ annual streamflow accumulation amounts and then multiplied by 100.
	Qmin1, Qmin7, Qmin30	m^3/s	Y, MY	Minimums of consecutive 1, 7, and 30 day~~s~~ streamflow averages (Olden and Poff, 2003).
	Q1st, Q5th, Q10th, Q25th, Q50th, Q75th, Q90th, Q95th, Q99th	m^3/s	Y, MY	The 1^{st}, 5^{th}, 10^{th}, 25^{th}, 50^{th} 75^{th}, 90^{th}, 95^{th}, and 99^{th} percentiles of daily streamflow (The Nature Conservancy, 2009; Olden and Poff, 2003). For example, *Q50th* means the median of streamflow time series.
	Qmean1, Qmean2, Qmean3, Qmean4, Qmean5, Qmean6, Qmean7, Qmean8, Qmean9, Qmean10, Qmean11, Qmean12, Qmean	m^3/s	Y, MY	Monthly and annual mean flows. For example, *Qmean6* means the ~~monthly~~ mean flow of June; *Qmean* is the annual mean flow.
	Qhigh, Qlow	m^3/s	MY	High and low flow event thresholds. *QHigh* equals 9 times *Q50th* (Clausen and Biggs, 2000); *Qlow* equals 0.2 times *Qmean* (Olden and Poff, 2003).
	RM, BM	m^3/s	Y	Runoff magnitude and baseflow magnitude. *RM* and *BM* are the differences between the maximum and minimum of streamflow and baseflow respectively (Horner, 2020).
Frequency	*FreH, FreL, FreZ*	-	Y	Frequencies of high flow (*FreH*), low flow (*FreL*), and zero flow (*FreZ*) days. *FreH* is the ratio of days with streamflow bigger than

Category	Index name	Units	Resolution	Definition
				Qhigh to the total days; *FreL* is the ratio of days with streamflow less than *Qlow* to the total days; *FreZ* is the ratio of days with zero streamflow to the total days (Addor et al., 2018).
	Fre1st, Fre5th, Fre95th, Fre99th	-	Y	Frequencies of days with streamflow bigger than or smaller than thresholds of the 1st, 5th, 95th, and 99th streamflow percentiles. *Fre1st /Fre5th* is the ratio of days in one year with streamflow less than the 1st/5th percentile of the whole multiyear streamflow time series to the days of one year; *Fre95th /Fre99th* is the ratio of days in one year with streamflow bigger than the 95th/99th percentile of the whole multiyear streamflow time series to the days of one year.
	NumH, NumL, NumZ	-	Y	Numbers of streamflow events with thresholds of *Qhigh*, *Qlow*, and zero (Olden and Poff, 2003).
	Num1st, Num5th, Num95th, Num99th	-	Y	Numbers of streamflow events with thresholds of the 1st, 5th, 95th, and the 99th percentile of the whole multiyear streamflow time series (Olden and Poff, 2003).
Duration	*DurH, DurL, DurZ,*	days	Y	Mean duration of streamflow events with thresholds of *Qhigh*, *Qlow*, and zero (Westerberg and Mcmillan, 2015).
	Dur1st, Dur5th, Dur95th, Dur99th	days	Y	Mean duration of streamflow events with thresholds of the 1st, 5th, 95th, and 99th percentiles of the whole multiyear streamflow time series.
Changing rate	*RBFI*	-	Y, MY	Richards-Baker flashiness index (Baker et al., 2004).
	RLD	-	Y, MY	Rising limb density (*RLD*) is a ratio of the number of rising limbs to the number of rising hydrograph (Sawicz et al., 2011).
	RRmean, RRmedian, FRmean, FRmedian	m^3/s	Y	*RRmean* and *RRmedian* are the mean and median of all positive differences between consecutive daily streamflow values in a year; *FRmean* and *FRmedian* are the mean and median of all negative differences between consecutive daily streamflow values in a year (The Nature Conservancy, 2009).
Timing	*FSS*	days since 1 January	Y, MY	*FSS* is the start date of flood season, which is defined as the start date of the consecutive 180 days whose streamflow average is the biggest in specific calendar year. It is calculated as the following: calculate a sliding average streamflow time series by applying sliding average method to the whole streamflow time series with a sliding window of 180 days; found the maximums of every calendar year in the averaged streamflow time series; start dates of corresponding sliding windows are *FSSs* of every calendar year.
	HFD	days	Y, MY	Half flow date (*HFD*) is the date on which half of a water year's total streamflow has passed since start of the water year (Court, 1962).
	HFI	days	Y, MY	Half flow interval (*HFI*) is the time span between the date on which a quarter of a water year's total streamflow has passed since start of the water year and the date on which three quarters of a water year's total streamflow has passed since start of the water year (Court, 1962).
	MMD	days since 1 January	Y, MY	Momentary maximum date (*MMD*) is the date when the maximum streamflow occurs (Court, 1962).
	MC7FD	days since 1 January	Y, MY	Minimum consecutive 7-day flow date (*MC7FD*) is the date when the minimum of consecutive 7-day flow averages occurs (Gudmundsson et al., 2018).
Variability	*VY*	-	Y, MY	Variance of ~~streamflow time series~~daily streamflow (Clausen and Biggs, 2000).
	COVY	-	Y, MY	Coefficient of variation of daily streamflow~~streamflow time series~~ (Clausen and Biggs, 2000).
	QCV	-	Y, MY	*QCV* means quartile-based coefficient of variation of daily streamflow~~streamflow time series~~, which is calculated as (*Q75th-Q25th*)/*Q50th*.
	RMM	-	Y, MY	Ratio of *Qmax1* to *Q50th*.
	GNC	-	Y, MY	Gini coefficient (Gudmundsson et al., 2018).
	SFDC	-	Y, MY	Slope of flow duration curve (*SFDC*) is the slope of flow duration curve between 33rd and 66th percentiles of streamflow (Mcmillan et al., 2017).
	SDP	-	MY	*SDP* is the slope of distribution of peaks, which is the slope between the 10th and 50th of a flow duration curve constructed by only includ~~consider~~ing hydrograph peaks (Euser et al., 2013).
	VI	-	Y, MY	Variability index (*VI*) is the standard deviation of the common logarithms of streamflow determined at 10% intervals from 10%

Category	Index name	Units	Resolution	Definition
				to 90% of the flow duration curve (Lane and Lei, 1950; Estrany et al., 2010).
Recession	*BFI*	-	Y, MY	Baseflow index (*BFI*) is the ratio of baseflow volume to streamflow volume over a specific time period (Singh et al., 2019).
	BRC	-	Y, MY	*BRC* is baseflow recession constant. Hydrograph recession assuming exponential recession behaviour is given by $Q_t = Q_0 e^{-kt}$, where Q_t is the streamflow at time t (day), Q_0 is the streamflow at the beginning of the recession, and k is the *BRC* (Safeeq et al., 2013). The master recession curve, which combines individual recession segments, is constructed by using the adapted matching strip method and then used for the calculation of *BRC* (Posavec et al., 2006).

Note: For most indices, the calculation on multi-year scale is using the same algorithm as the calculation on yearly scale ~~-~~except that the used time series is the whole multi-year time series rather than one year's segment. For indices including FSS, HFD, HFI, MMD, and MC7FD, the multi-year values are the medians of yearly values.

3.2 Quality flags of yearly indices

According to the quality of streamflow records used for indices calculation, every yearly index value is accompanied by a quality flag for quality control. The purpose that we define the flags is to provide a space for individuals with different research objectives to have a free choice. They can use only the highest-quality indices values out of caution, or they can take some risks and add some relatively low-quality indices values in order to increase the sample size. Quality flags of yearly indices values were determined according to corresponding streamflow records and the same criteria as is shown in Table 3.

~~1.4~~3.3 Example streamflow indices time series

To give a first impression of streamflow indices time series, Fig. 4 shows some ~~example~~ streamflow indices time series ~~for the seven components of the streamflow regime~~ of Nashwaak River at Durham Bridge, Canada ~~at yearly resolution~~on a yearly scale as an example. It is obvious that the *Qmax1* and *Qmean* are~~is~~ increasing ~~as well as the *Qmean*~~ while *Qmin7* has no obvious trend. The *RM* also shows~~, which accompanies~~ an upward trend ~~of *RM*~~. These trends indicate that the magnitude of high flow is increasing. Moreover, the *Num99th* and *Dur99th* are also increasing, which means the number and lasting time of flood are rising too. To make matters worse, the *RBFI* and *RRmean* are obviously climbing as well~~, too~~. ~~In contrast, the *FRmean* is decreasing.~~ It means the streamflow regime of Nashwaak River is becoming more and more flashy with a higher rising-dropping speed of floods. Besides, the *BFI* also shows a downward trend, which indicates worse flow regulations of the river basin. In conclusion, ~~these shifts of the streamflow regime components show that~~ the floods have grown in intensity and therefore flood forecasting and protection are becoming more important there.

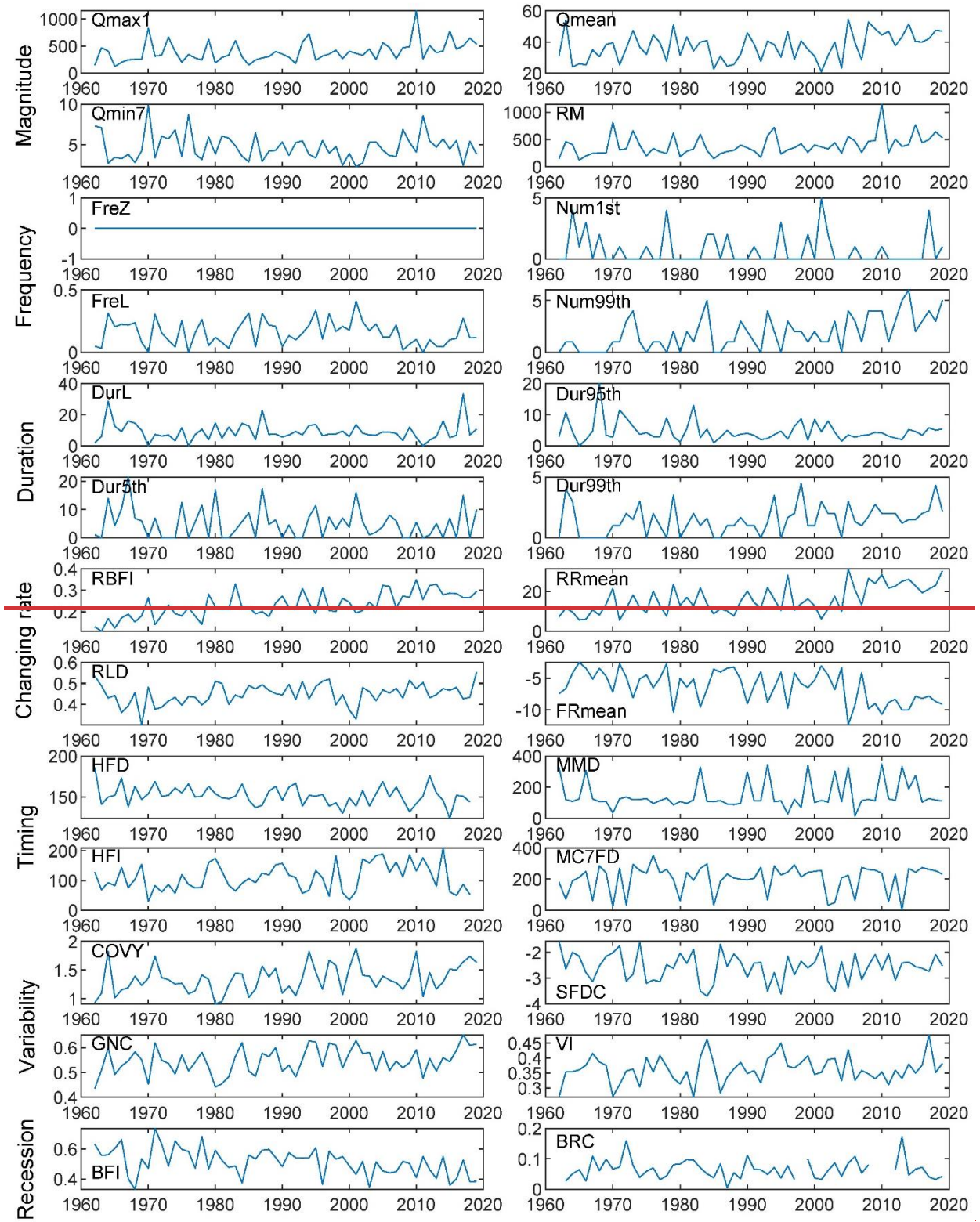
Magnitude
Qmax1
Qmean
Qmin7
RM
Frequency
FreZ
Num1st
FreL
Num99th
Duration
DurL
Dur95th
Dur5th
Dur99th
Changing rate
RBFI
RRmean
RLD
FRmean
Timing
HFD
MMD
HFI
MC7FD
Variability
COVY
SFDC
GNC
VI
Recession
BFI
BRC

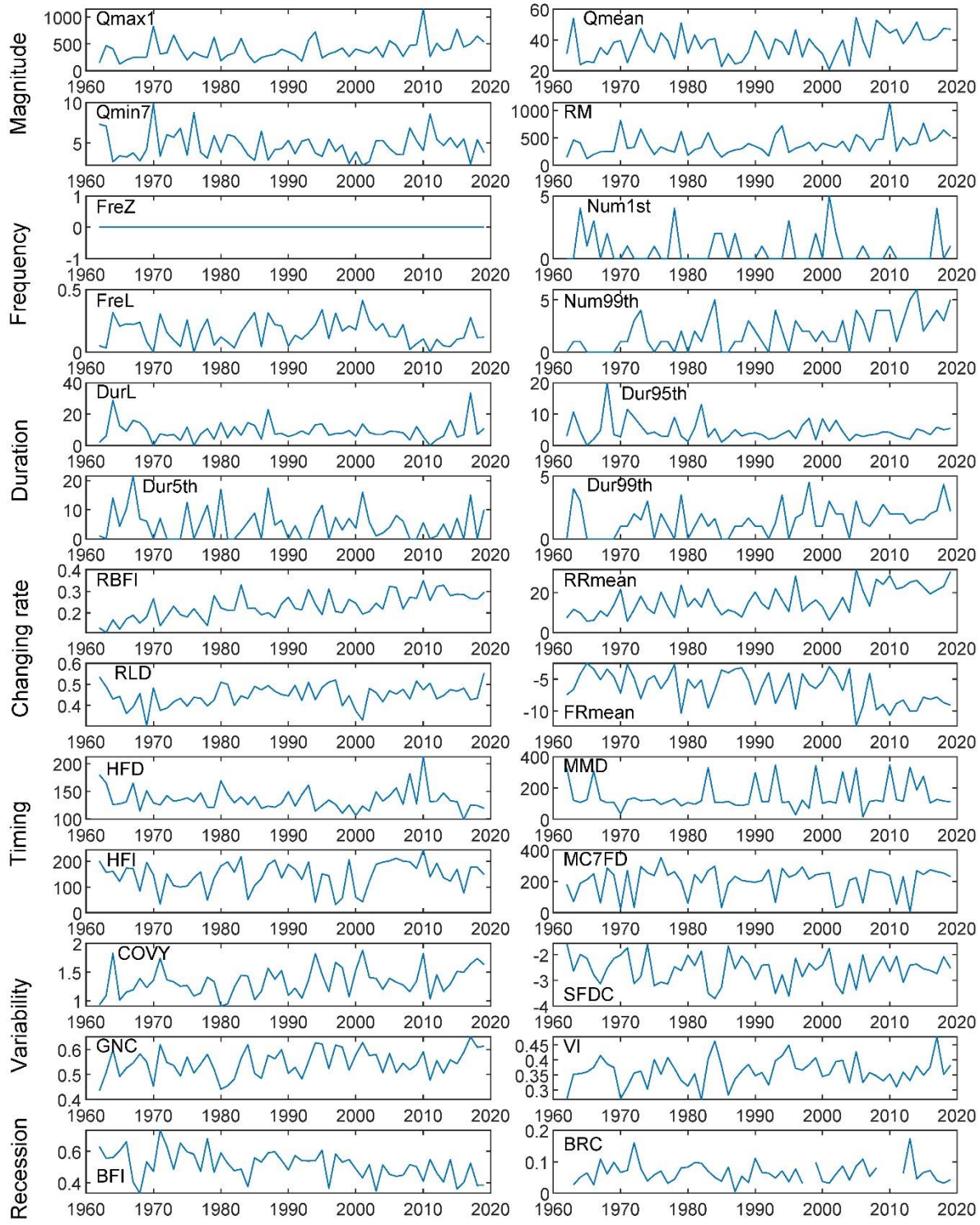

360 **Figure 4. Example streamflow indices time series for seven components of the streamflow regime of Nashwaak River at Durham Bridge, Canada ~~at yearly resolution~~on a yearly scale. R~~Please r~~efer to Table ~~4~~1 for the definitions ~~names~~ and units of indices.**

4 A comparative analysis~~An exemplary application~~

Studies on streamflow regime on a global scale are mainly focused on the magnitude of streamflow. There are few or even no global-scale studies on other components of streamflow regime. Therefore, several studies' results about trends in annual mean
365 and extreme streamflow were selected for comparisons with our dataset's. Figure 5 shows trends in yearly indices of mean and extreme streamflow during 1970 to 2022 derived from our dataset. Noticeable clusters of upward trends in annual mean streamflow appear in the east part of the US near the Great Lakes and the northwest part of Europe (Figure 5a). The results are in accord with the results of Gudmundsson et al. (2019) and Yang et al. (2021) but show more details as our collection have

more stations (more than 40000 stations) compared to around 30000 stations of Gudmundsson et al. (2019) and around 20000 stations of Yang et al. (2021). The spatial pattern of annual maximum streamflow is also in line with those in Do et al. (2017) and Yin et al. (2018)'s papers but have a higher resolution because a larger number of stations are included (Figure 5f). It is noticeable that the signs of trends in different percentiles and mean of streamflow are consistent in most of regions. When one index shows an upward trend, it is highly probable that other indices will also exhibit an upward trend, and vice versa. However, there are some differences between the magnitude of changes in different indices values. The absolute values of relative change per decade of Qmin1 are obviously larger than those of other indices (Figure 5b). In contrast, the absolute values of relative change per decade of Qmax1 are noticeably smaller than those of other indices (Figure 5f). As the percentile increases, the absolute value of relative change per decade tends to decrease. It indicates that the low flow is more sensitive to the changing environment compared to high flow. The low flow of rivers is more vulnerable to the threat of drying up, and the regulation of streamflow during low flow period should be strengthened to ensure the ecological functions as well as water supply. (Gudmundsson et al., 2019; Yin et al., 2018; Yang et al., 2021; Do et al., 2017; Wasko et al., 2020; Beck et al., 2015)

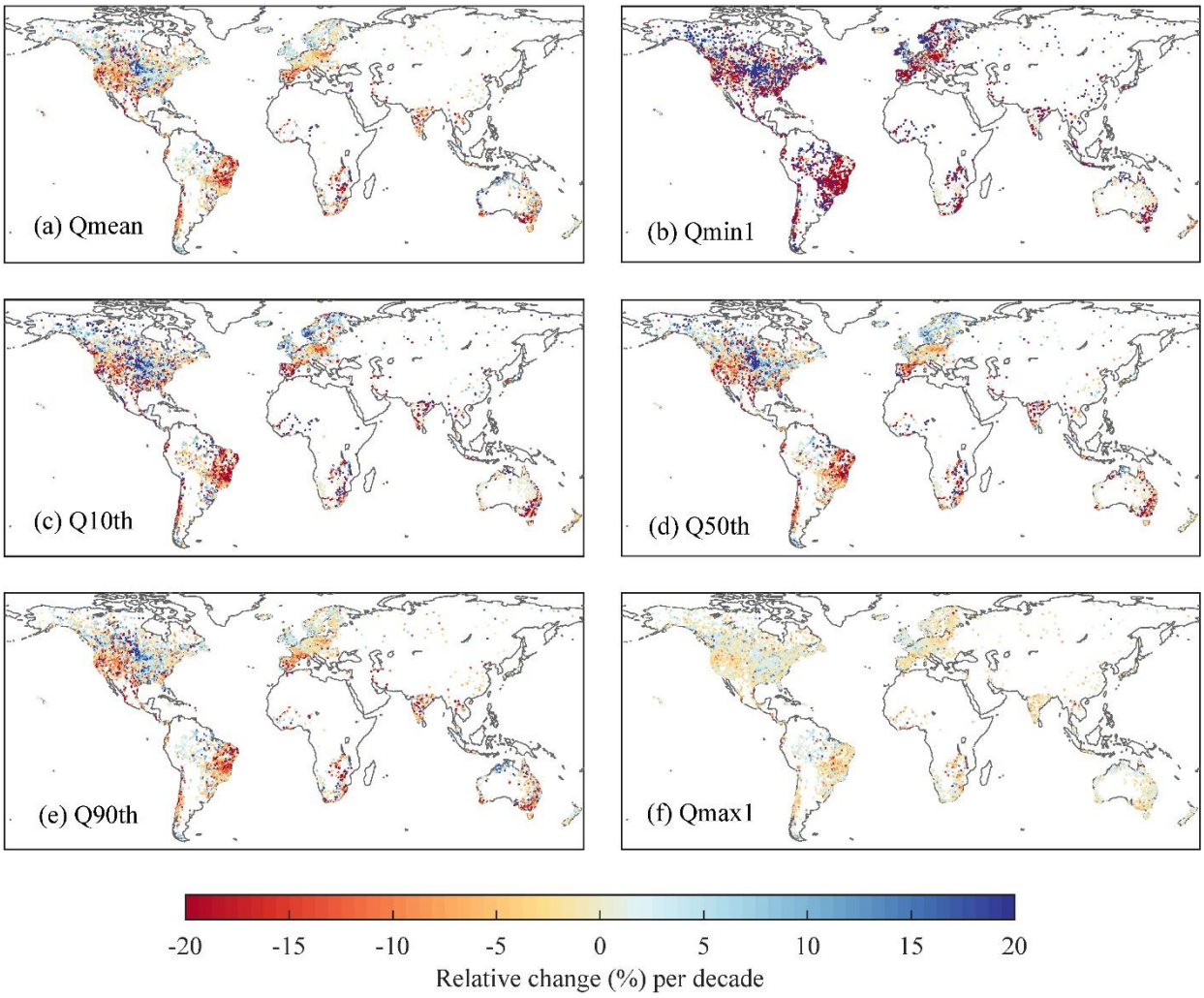

Figure 5. Trends in annual mean and percentiles of streamflow during 1970 to 2022. Relative change per decade is the trend in yearly index multiplied by ten years and then divided by the multi-year index value. The trends were calculated using Sen's slope estimator. See Gocic and Trajkovic (2013) for details. Refer to Table 4 for the definitions of indices.

~~An example investigation into the trend and abrupt change of temporal concentration of streamflow on a global scale has been done to illustrate a use of the streamflow indices time series dataset. Fig. 5 shows the trends and abrupt change points of half-flow interval (HFI) time series on a global scale with a 95% confidence level. The trends were tested using the Mann-Kendall trend test (Kendall, 1948) and calculated using the Sen's slope method (Sen, 1968).The abrupt change points were detected by~~

~~combining the results of Pettitt test (Pettitt, 1979) and the heuristic segmentation algorithm (Bernaola-Galván et al., 2001) after detrending. The HFI is an index that quantifies the temporal concentration of streamflow. A small HFI means a half of yearly discharge is generated in a short time, and thus reflects a concentrated streamflow regime. It is obvious that near and in the Arctic, almost all rivers' HFIs show significant upward trends, which means streamflow of those rivers has been less temporally concentrated (Fig. 5a). Feng et al. (2021) found that the zero flow days of Arctic rivers are declining strongly, while the yearly discharge accelerations altered very slightly, which implies that the streamflow of Arctic rivers is becoming more evenly distributed within a water year. The causes are likely the reservoir operations and the earlier snowmelt because of the climate change (Tan et al., 2011; Suzuki et al., 2020; Adam et al., 2007).~~

~~It is also noticeable that in the northern part of Australia, the HFIs tend to have an upward trend, while in the southern part, the HFIs tend to have a downward trend. Actually, there is a downward trend in annual total rainfall in southern part of Australia and a upward trend in northern part of Australia, and the trend pattern of annual total streamflow is the same as annual total rainfall (Zhang et al., 2014; Zhang et al., 2016). The trends of HFIs in Australia are probably due to the change of precipitation, but the cause of the change of precipitation is still under discussion (Dey et al., 2019). Besides, there are clusters of significant trends of HFIs in the US, middle part of South America, South Africa, Europe, China, and India. There are also clusters of significant abrupt change points of HFIs as shown in Fig. 5b. In South America, a cluster of significant abrupt change points occurs in 2010 to 2019, which may be attributed to the strong tropical Atlantic warming and tropical Pacific cooling as well as the deforestation (Barichivich et al., 2018). In Europe, most of the significant abrupt change points are before 1970. indicated that strong shifts in the streamflow patterns on a continental scale have occurred in Europe after around 1960, which agrees with our finding. Actually, Europe has experienced pronounced changes inclimate (Fontrodona Bach et al., 2018) and land cover (urbanization, reforestation, and afforestation; see Fuchs et al. (2013)) since the 1960s, which probably caused the abrupt change points.~~

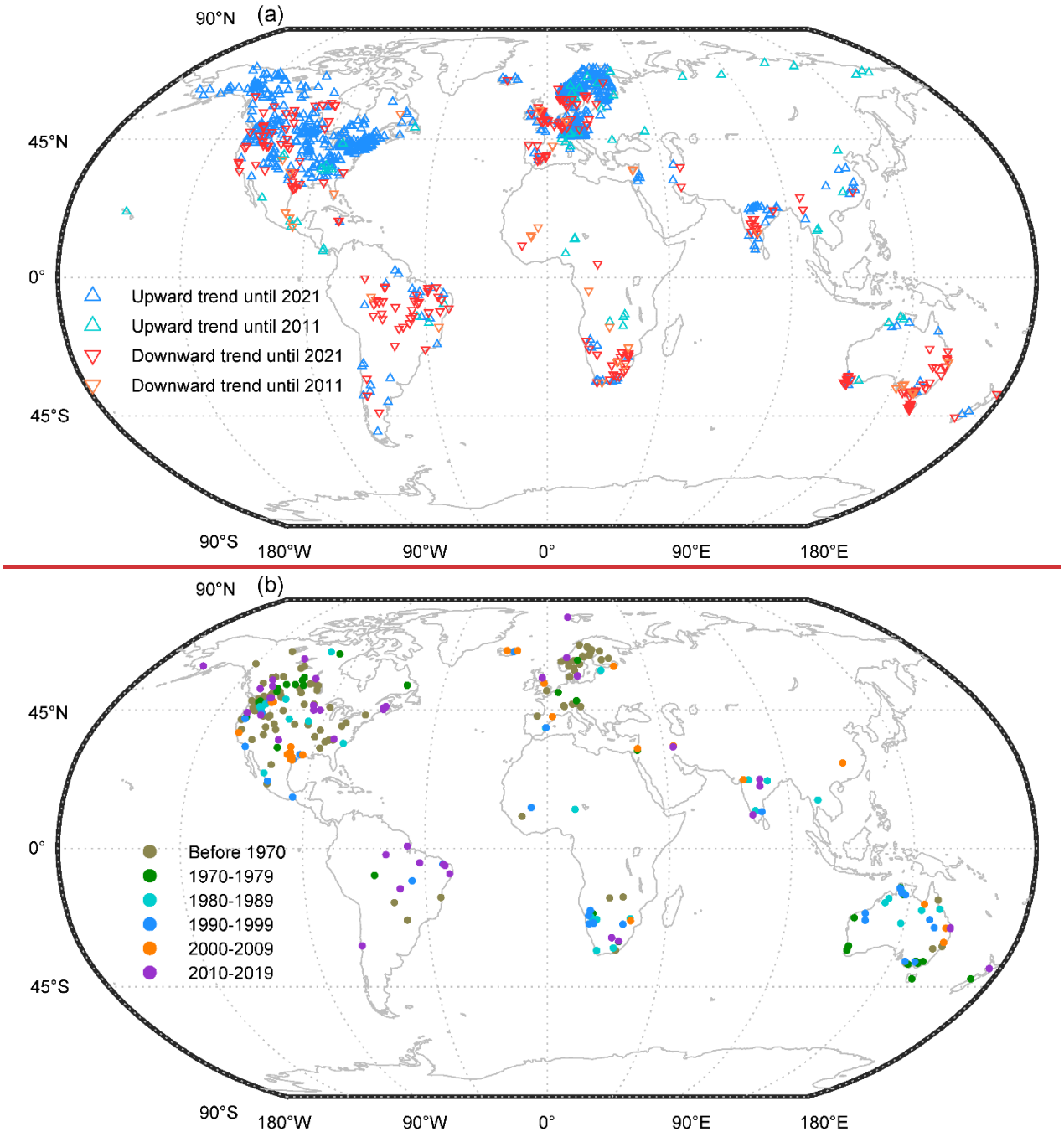

~~**Figure 5. The (a) trends and (b) abrupt change points of half-flow interval time series on a global scale. All data shown have passed the significance test with a 95% confidence level.**~~

5 Data availability

The global streamflow indices time series dataset is available for download at https://doi.org/10.57760/sciencedb.07227 ~~https://www.scidb.cn/en/s/M32eEb~~ (Chen et al., 2023a)~~(Chen et al. 2023)~~. There are two folders corresponding to two different data storage ways. One is "MAT" for the files with .mat extension, which is a binary data container format used in the MATLAB. The other is "CSV" for the files with .csv extension, in which the data are stored as a delimiter-separated text format. Apart from these, there is a file named "station_catalogue.csv". It contains the basic information and multi-year streamflow indices of every hydrological station. ~~There are two folders corresponding to two different data storage ways. One is "MAT" for the files with ".mat" extension, which are a binary data container format used in the MATLAB. The other is "CSV" for the files with ".csv" extension, in which the data are stored as a delimiter-separated text format. Apart from these,~~

there is a file named "station_catalogue.csv". It contains the basic information and multi-year streamflow indices of every hydrological station and corresponding river reach (Table 25).

425

Table 25. The fields and definitions in "station_catalogue.csv".

Field	Definition
no	station ID number
no_ori	station ID number in the original data source
database	the database where records come from
river	river name
station	station name
country	country code (ISO 3166)
latitude	latitude (decimal degree)
longitude	longitude (decimal degree)
area	contributing area upstream of the gauge location (if available) in square kilometre
altitude	height of gauge above sea level (meter)
start	the start year of the time series
end	the end year of the time series
years	length of time series; years = end - start + 1
miss	percentage of missing values in original streamflow records (%)
flag	quality flag of station; see relevant paper for details
Qmax1	the maximum of daily streamflow (cubic meter per second)
MMD	date when Qmax1 occurred
Qmax3	the maximum of consecutive 3-day streamflow averages (cubic meter per second)
Qmax7	the maximum of consecutive 7-day streamflow averages (cubic meter per second)
Qmax30	the maximum of consecutive 30-day streamflow averages (cubic meter per second)
Qmin1	the minimum of daily streamflow (cubic meter per second)
Qmin7	the minimum of consecutive 7-day streamflow averages (cubic meter per second)
MC7FD	the first day of consecutive 7 days of Qmin7
Qmin30	the minimum of consecutive 30-day streamflow averages (cubic meter per second)
Q1st	the 1st percentile of daily streamflow (cubic meter per second)
Q5th	the 5th percentile of daily streamflow (cubic meter per second)
Q10th	the 10th percentile of daily streamflow (cubic meter per second)
Q25th	the 25th percentile of daily streamflow (cubic meter per second)
Q50th	the 50th percentile of daily streamflow (cubic meter per second)
Q75th	the 75th percentile of daily streamflow (cubic meter per second)
Q90th	the 90th percentile of daily streamflow (cubic meter per second)
Q95th	the 95th percentile of daily streamflow (cubic meter per second)
Q99th	the 99th percentile of daily streamflow (cubic meter per second)
Qmean	long-term average discharge (cubic meter per second)
Qmean1	the long-term average discharge in January (cubic meter per second)
Qmean2	the long-term average discharge in February (cubic meter per second)
Qmean3	the long-term average discharge in March (cubic meter per second)
Qmean4	the long-term average discharge in April (cubic meter per second)

Field	Definition
Qmean5Q90th	the long-term average discharge in May (cubic meter per second) the 90th percentile of daily streamflow (m3/s)
Qmean6Q95th	the long-term average discharge in June (cubic meter per second) the 95th percentile of daily streamflow (m3/s)
Qmean7Q99th	the long-term average discharge in July (cubic meter per second) the 99th percentile of daily streamflow (m3/s)
Qmean8Qhigh	the long-term average discharge in August (cubic meter per second) high flow event threshold (m3/s)
Qmean9Qlow	the long-term average discharge in September (cubic meter per second) low flow event threshold (m3/s)
Qmean10RBFI	the long-term average discharge in October (cubic meter per second) Richards-Baker flashiness index
Qmean11RLD	the long-term average discharge in November (cubic meter per second) rising limb density
Qmean12FSS	the long-term average discharge in December (cubic meter per second) the start month of flood season
QhighHFD	high flow event threshold (cubic meter per second) half flow date (days)
QlowHFI	low flow event threshold (cubic meter per second) half flow interval (days)
RBFIMMD	Richards-Baker flashiness index momentary maximum date (days since 1 January)
RLDMC7FD	rising limb density minimum consecutive 7-day flow date (days since 1 January)
FSSVY	the start month of flood season variance of streamflow time series
HFDCOVY	half flow date (days) coefficient of variation of streamflow time series
HFIQCV	half flow interval (days) quartile-based coefficient of variation of streamflow time series
VYRMM	variance of streamflow time series ratio of maximum to median of streamflow time series
COVYGNC	coefficient of variation of streamflow time series Gini coefficient
QCVSFDC	quartile-based coefficient of variation of streamflow time series slope of flow duration curve
RMMSDP	ratio of maximum to median of streamflow time series slope of distribution of peaks
GNCVI	Gini coefficient variability index
SFDCBFI	slope of flow duration curve baseflow index
SDPBRC	slope of distribution of peaks baseflow recession constant

6 Conclusions and perspective

This paper presents a new global discharge streamflow indices time series dataset for large-sample hydrology, whichand is designed to characterize the especially beneficial for hydrological analysis on streamflow regime comprehensively. It includes 79 indices over 7 components of streamflow regime (*i.e.*, magnitude, frequency, duration, changing rate, timing, variability, and recession) of 4126355548 river reaches globally on yearly and multiyear scales. Before the establishmentbuild of indices indices dataset, streamflow records and metadata from nine databases were collected and merged into one data collection. Data quality control was performed by removing duplicate and unreasonable records, and attaching quality flags to all records and stations. Quality flags were also attached to each yearly index value in the indices dataset. A comparative analysis was performed on the trends in annual mean and percentiles of streamflow on a global scale. The results show that our dataset's results are in accord with the results of existing studies, but our results have a higher resolution because a larger number of stations are included. Our results also indicate that the low flow is more sensitive to the changing environment compared to high flow.

the data collection of 15408 hydrological stations was constructed with data from GRDC, WRIS, ArcticGRO, and CHY. After that, data quality control was done on the data collection by applying an automatic detection method to identify and modify unreasonable values and to remove stations with record length less than 30 years as well as stations with the latest streamflow record date before 2000. A simple investigation into the trend and abrupt change of temporal concentration of streamflow on a global scale was conducted as a use case of the streamflow indices dataset. Significant clusters are found in both trends and abrupt changes globally. Further investigations are needed to reveal the causes, which is beyond the scope of this study.

Compared to available similarexisting datasets, ourthe new indices dataset has several advantages. Firstly, it includes more indices, which canould characterize streamflow regime more comprehensively. In contrast withO widely used GSIM, the newur indices dataset covers indices that characterize the frequency, duration, changing rate, and recession of streamflow

regime, which are not included in GSIM or completely incorporated in other global-scale datasets. To the best of our knowledge, our dataset is the most comprehensive global-scale indices dataset in terms of streamflow indices coverage. ~~.~~ ~~-~~Secondly, it includes a larger number (41263) of stations with longer time series (from 1806 to 2022) compared to existing streamflow indices datasets. By comparison, GSIM includes 30959 stations with yearly indices time series from 1806 to 2016. The additional stations are mainly located in the US and China.

~~new river reaches and their hydrological data, especially the restricted-access hydrological data in China are included. The 33 hydrological stations cover typical river reaches of 7 largest river basins in China. Thirdly, it has longer time series which ends up no earlier than 2000. The new indices dataset has indices characterizing the frequency, duration, changing rate, and recession of streamflow regime, which are very important indices to study, for example, flow regime changes.~~ This dataset will greatly facilitate large-sample studies on both global and regional scales on a great number of hydrological issues related to streamflow regime, such as:~~As for the indices of magnitude, timing, and variability, the new indices dataset includes more indices, representing more comprehensive characterizing of such streamflow components. For example, the slope of flow duration curve, slope of distribution of peaks, and variability index, which represent the variability of seasonal water balance, peak discharges, and flow duration curve respectively, are included in the new dataset.~~ (1) calibration, evaluation, and improvement of hydrological models for water resource assessment; (2) estimation of impacts of factors (like vegetation greening and snow melting caused by climate change) on streamflow regime components; (3) construction, training, and evaluation of machine learning models for hydrological forecasting and catchment classification; (4) assessment of impacts of streamflow regime shifts on biogeochemical cycles (like soil erosion) and ecological functions of streamflow; (5) analysis on the spatiotemporal pattern of streamflow regime shifts and attribution; and (6) identification of nonstationary of streamflow indices and its attribution.

~~The indices time series in the new dataset are available till 2021, with lengths varying from 30 to 215 years and an average length of around 66 years. By comparison, taking GSIM as an example, the indices time series in GSIM are between 1806 and 2016 with lengths varying from 1 to 208 years and an average length of around 38 years. Besides, more than 3500 stations' indices time series of the new dataset are available after 2017. With regard to China's hydrological data, most other datasets neither include such number of stations nor the latest records in the past two decades. For instance, all indices time series of GSIM are not available after 2004 and the time spans are from 1947 to 2004 with an average length of 12 years. Comparatively, all indices time series of this new dataset are available until 2020 and the time spans are from 1947 to 2020 with an average length of 54 years.~~(Beck et al., 2015; Gudmundsson et al., 2018; Tramblay et al., 2021; Yang et al., 2021; Yin et al., 2023)

~~This new dataset is more comprehensive and covers most common indices for streamflow regime analyses on a global scale. With the dataset, large-sample studies, such as research on streamflow regime, will become easier without spending time collecting and handling raw streamflow records.~~ ~~This new dataset is a valuable source to the hydrology community to fill the gap of research on the variability, timing, changing rate, etc. of daily streamflow from a big-picture perspective. Moreover, in some cases related to hydrological risks analysis, catchment classification, hydrological model calibration and so on, the new dataset can be also useful if no original records are available.~~

Author contribution

LJ conceived the idea. LJ and XC conceptualized the study. XC, YL and LJ curated the data; XC compiled the data, performed the analyses and produced the figures; All authors contributed to the original draft of the paper.

Competing interests

The contact author has declared that neither they nor their co-authors have any competing interests.

Acknowledgements

The authors wish to express their gratitude to all the data providers, *i.e.*, the Global Runoff Data Centre (GRDC), U.S. Geological Survey (USGS), Water Survey of Canada (HYDAT), National Water Agency of Brazil (ANA), the Chilean Center for Climate and Resilience Research (CCCRR), Woodwell Climate Research Centre (ArcticGRO), Ministry of Water Resources of China (CHY), Central Water Commission of India (WRIS), and Australian Bureau of Meteorology (BOM), ~~the India Water Resources Information System (WRIS), and the Arctic Great Rivers Observatory (ArcticGRO)~~ for their ~~efforts~~ in archiving streamflow observations and sharing the data ~~publicly~~. The authors are also grateful to the developers of TOSSH toolbox for providing such a useful tool and ~~to~~ Alex Buzacott for sharing a R package to download Australian water data at https://github.com/buzacott/bomWater. ~~The~~ The help from Rongrong Li from Wuhan University is highly appreciated for collecting streamflow data.

Financial support

This study is financially supported by the research startup grants (Y01296129; Y01296229).

References

Adam, J. C., Haddeland, I., Su, F., and Lettenmaier, D. P.: Simulation of reservoir influences on annual and seasonal streamflow changes for the Lena, Yenisei, and Ob'rivers, Journal of Geophysical Research: Atmospheres, 112, 2007.

Addor, N., Newman, A. J., Mizukami, N., and Clark, M. P.: The CAMELS data set: catchment attributes and meteorology for large-sample studies, Hydrol. Earth Syst. Sci., 21, 5293-5313, 10.5194/hess-21-5293-2017, 2017.

Addor, N., Do, H. X., Alvarez-Garreton, C., Coxon, G., Fowler, K., and Mendoza, P. A.: Large-sample hydrology: recent progress, guidelines for new datasets and grand challenges, Hydrological Sciences Journal, 65, 712-725, 2020.

Addor, N., Nearing, G., Prieto, C., Newman, A., Le Vine, N., and Clark, M. P.: A ranking of hydrological signatures based on their predictability in space, Water Resources Research, 54, 8792-8812, 2018.

Alvarez-Garreton, C., Mendoza, P. A., Boisier, J. P., Addor, N., Galleguillos, M., Zambrano-Bigiarini, M., Lara, A., Puelma, C., Cortes, G., and Garreaud, R.: The CAMELS-CL dataset: catchment attributes and meteorology for large sample studies–Chile dataset, Hydrology and Earth System Sciences, 22, 5817-5846, 2018.

Baker, D. B., Richards, R. P., Loftus, T. T., and Kramer, J. W.: A new flashiness index: Characteristics and applications to midwestern rivers and streams, JAWRA Journal of the American Water Resources Association, 40, 503-522, 2004.

Barichivich, J., Gloor, E., Peylin, P., Brienen, R. J. W., Schöngart, J., Espinoza, J. C., and Pattnayak, K. C.: Recent intensification of Amazon flooding extremes driven by strengthened Walker circulation, Science Advances, 4, eaat8785, 10.1126/sciadv.aat8785, 2018.

Beck, H. E., de Roo, A., and van Dijk, A. I. J. M.: Global Maps of Streamflow Characteristics Based on Observations from Several Thousand Catchments, Journal of Hydrometeorology, 16, 1478-1501, https://doi.org/10.1175/JHM-D-14-0155.1, 2015.

Bernaola-Galván, P., Ivanov, P. C., Nunes Amaral, L. A., and Stanley, H. E.: Scale Invariance in the Nonstationarity of Human Heart Rate, Physical Review Letters, 87, 168105, 10.1103/PhysRevLett.87.168105, 2001.

Botter, G., Basso, S., Rodriguez-Iturbe, I., and Rinaldo, A.: Resilience of river flow regimes, Proceedings of the National Academy of Sciences, 110, 12925-12930, doi:10.1073/pnas.1311920110, 2013.

Brouziyne, Y., De Girolamo, A. M., Aboubdillah, A., Benaabidate, L., Bouchaou, L., and Chehbouni, A.: Modeling alterations in flow regimes under changing climate in a Mediterranean watershed: An analysis of ecologically-relevant hydrological indicators, Ecological Informatics, 61, 101219, https://doi.org/10.1016/j.ecoinf.2021.101219, 2021.

Chagas, V. B., Chaffe, P. L., Addor, N., Fan, F. M., Fleischmann, A. S., Paiva, R. C., and Siqueira, V. A.: CAMELS-BR: hydrometeorological time series and landscape attributes for 897 catchments in Brazil, Earth System Science Data, 12, 2075-2096, 2020.

Chen, X., Jiang, L., Luo, Y., and Liu, J.: A global streamflow indices time series dataset, Science Data Bank. [dataset], https://doi.org/10.57760/sciencedb.07227., 2023a.

Chen, X., Quan, Q., Zhang, K., and Wei, J.: Spatiotemporal characteristics and attribution of dry/wet conditions in the Weihe River Basin within a typical monsoon transition zone of East Asia over the recent 547 years, Environmental Modelling & Software, 143, 105116, https://doi.org/10.1016/j.envsoft.2021.105116, 2021.

Chen, X., Zhang, K., Luo, Y., Zhang, Q., Zhou, J., Fan, Y., Huang, P., Yao, C., Chao, L., and Bao, H.: A distributed hydrological model for semi-humid watersheds with a thick unsaturated zone under strong anthropogenic impacts: a case study in Haihe River Basin, Journal of Hydrology, 129765, https://doi.org/10.1016/j.jhydrol.2023.129765, 2023b.

Cheng, Y., Sang, Y., Wang, Z., Guo, Y., and Tang, Y.: Effects of Rainfall and Underlying Surface on Flood Recession—The Upper Huaihe River Basin Case, International Journal of Disaster Risk Science, 12, 111-120, 10.1007/s13753-020-00310-w, 2021.

Clark, M. P., Rupp, D. E., Woods, R. A., Tromp‐van Meerveld, H., Peters, N., and Freer, J.: Consistency between hydrological models and field observations: linking processes at the hillslope scale to hydrological responses at the watershed scale, Hydrological Processes: An International Journal, 23, 311-319, 2009.

Clausen, B. and Biggs, B.: Flow variables for ecological studies in temperate streams: groupings based on covariance, Journal of hydrology, 237, 184-197, 2000.

Colls, M., Timoner, X., Font, C., Sabater, S., and Acuña, V.: Effects of Duration, Frequency, and Severity of the Non-flow Period on Stream Biofilm Metabolism, Ecosystems, 22, 1393-1405, 10.1007/s10021-019-00345-1, 2019.

Court, A.: Measures of streamflow timing, Journal of Geophysical Research, 67, 4335-4339, 1962.

Coxon, G., Addor, N., Bloomfield, J. P., Freer, J., Fry, M., Hannaford, J., Howden, N. J. K., Lane, R., Lewis, M., Robinson, E. L., Wagener, T., and Woods, R.: CAMELS-GB: hydrometeorological time series and landscape attributes for 671 catchments in Great Britain, Earth Syst. Sci. Data, 12, 2459-2483, 10.5194/essd-12-2459-2020, 2020.

Crochemore, L., Isberg, K., Pimentel, R., Pineda, L., Hasan, A., and Arheimer, B.: Lessons learnt from checking the quality of openly accessible river flow data worldwide, Hydrological Sciences Journal, 65, 699-711, 10.1080/02626667.2019.1659509, 2020.

Cushman, R. M.: Review of Ecological Effects of Rapidly Varying Flows Downstream from Hydroelectric Facilities, North American Journal of Fisheries Management, 5, 330-339, 10.1577/1548-8659(1985)5<330:ROEEOR>2.0.CO;2, 1985.

Delaigue, O., Brigode, P., Andréassian, V., Perrin, C., Etchevers, P., Soubeyroux, J.-M., Janet, B., and Nans, A.: CAMELS-FR: A large sample hydroclimatic dataset for France to explore hydrological diversity and support model benchmarking, IAHS-2022 Scientific Assembly,

Dey, R., Lewis, S. C., Arblaster, J. M., and Abram, N. J.: A review of past and projected changes in Australia's rainfall, WIREs Climate Change, 10, e577, https://doi.org/10.1002/wcc.577, 2019.

Do, H. X., Westra, S., and Leonard, M.: A global-scale investigation of trends in annual maximum streamflow, Journal of Hydrology, 552, 28-43, https://doi.org/10.1016/j.jhydrol.2017.06.015, 2017.
Do, H. X., Gudmundsson, L., Leonard, M., and Westra, S.: The Global Streamflow Indices and Metadata Archive (GSIM) – Part 1: The production of a daily streamflow archive and metadata, Earth Syst. Sci. Data, 10, 765-785, 10.5194/essd-10-765-2018, 2018.
Ebeling, P., Kumar, R., Lutz, S. R., Nguyen, T., Sarrazin, F., Weber, M., Büttner, O., Attinger, S., and Musolff, A.: QUADICA: water QUAlity, DIscharge and Catchment Attributes for large-sample studies in Germany, Earth System Science Data, 14, 3715-3741, 2022.
Estrany, J., Garcia, C., and Batalla, R. J.: Hydrological response of a small mediterranean agricultural catchment, Journal of Hydrology, 380, 180-190, 2010.
Euser, T., Winsemius, H., Hrachowitz, M., Fenicia, F., Uhlenbrook, S., and Savenije, H.: A framework to assess the realism of model structures using hydrological signatures, Hydrology and Earth System Sciences, 17, 1893-1912, 2013.
Feng, D., Gleason, C. J., Lin, P., Yang, X., Pan, M., and Ishitsuka, Y.: Recent changes to Arctic river discharge, Nature Communications, 12, 6917, 10.1038/s41467-021-27228-1, 2021.
Fontrodona Bach, A., van der Schrier, G., Melsen, L. A., Klein Tank, A. M. G., and Teuling, A. J.: Widespread and Accelerated Decrease of Observed Mean and Extreme Snow Depth Over Europe, Geophysical Research Letters, 45, 12,312-312,319, https://doi.org/10.1029/2018GL079799, 2018.
Fowler, K. J., Acharya, S. C., Addor, N., Chou, C., and Peel, M. C.: CAMELS-AUS: hydrometeorological time series and landscape attributes for 222 catchments in Australia, Earth System Science Data, 13, 3847-3867, 2021.
Fuchs, R., Herold, M., Verburg, P., and Clevers, J. G. P. W.: A high-resolution and harmonized model approach for reconstructing and analysing historic land changes in Europe, Biogeosciences, 10, 1543-1559, 10.5194/bg-10-1543-2013, 2013.
Gehrke, P. C., Brown, P., Schiller, C. B., Moffatt, D. B., and Bruce, A. M.: River regulation and fish communities in the Murray-Darling river system, Australia, Regulated Rivers: Research & Management, 11, 363-375, https://doi.org/10.1002/rrr.3450110310, 1995.
Gnann, S. J., McMillan, H. K., Woods, R. A., and Howden, N. J. K.: Including Regional Knowledge Improves Baseflow Signature Predictions in Large Sample Hydrology, Water Resources Research, 57, e2020WR028354, https://doi.org/10.1029/2020WR028354, 2021a.
Gnann, S. J., Coxon, G., Woods, R. A., Howden, N. J., and McMillan, H. K.: TOSSH: A toolbox for streamflow signatures in hydrology, Environmental Modelling & Software, 138, 104983, 2021b.
Gocic, M. and Trajkovic, S.: Analysis of changes in meteorological variables using Mann-Kendall and Sen's slope estimator statistical tests in Serbia, Global and Planetary Change, 100, 172-182, https://doi.org/10.1016/j.gloplacha.2012.10.014, 2013.
Goeking, S. A. and Tarboton, D. G.: Variable Streamflow Response to Forest Disturbance in the Western US: A Large-Sample Hydrology Approach, Water Resources Research, 58, e2021WR031575, https://doi.org/10.1029/2021WR031575, 2022.
Gudmundsson, L. and Seneviratne, S. I.: Observation-based gridded runoff estimates for Europe (E-RUN version 1.1), Earth Syst. Sci. Data, 8, 279-295, 10.5194/essd-8-279-2016, 2016.
Gudmundsson, L., Do, H. X., Leonard, M., and Westra, S.: The Global Streamflow Indices and Metadata Archive (GSIM) – Part 2: Quality control, time-series indices and homogeneity assessment, Earth Syst. Sci. Data, 10, 787-804, 10.5194/essd-10-787-2018, 2018.
Gudmundsson, L., Leonard, M., Do, H. X., Westra, S., and Seneviratne, S. I.: Observed trends in global indicators of mean and extreme streamflow, Geophysical Research Letters, 46, 756-766, 2019.
Gudmundsson, L., Boulange, J., Do, H. X., Gosling, S. N., Grillakis, M. G., Koutroulis, A. G., Leonard, M., Liu, J., Müller Schmied, H., Papadimitriou, L., Pokhrel, Y., Seneviratne, S. I., Satoh, Y., Thiery, W., Westra, S., Zhang, X., and Zhao, F.: Globally observed trends in mean and extreme river flow attributed to climate change, Science, 371, 1159-1162, 10.1126/science.aba3996, 2021.
Gupta, H. V., Perrin, C., Blöschl, G., Montanari, A., Kumar, R., Clark, M., and Andréassian, V.: Large-sample hydrology: a need to balance depth with breadth, Hydrol. Earth Syst. Sci., 18, 463-477, 10.5194/hess-18-463-2014, 2014.
Harmon, B., Logan, L., Spiese, C., and Rahrig, R.: Flow alterations in rivers due to unconventional oil and gas development in the Ohio River basin, The Science of the total environment, 856, 159126, 10.1016/j.scitotenv.2022.159126, 2022.
Horner, I.: Design and evaluation of hydrological signatures for the diagnostic and improvement of a process-based distributed hydrological model, Université Grenoble Alpes, 2020.
Jacobson, R., Bouska, K., Bulliner, E., Lindner, G., and Paukert, C.: Geomorphic Controls on Floodplain Connectivity, Ecosystem Services, and Sensitivity to Climate Change: An Example From the Lower Missouri River, Water Resources Research, 58, 10.1029/2021WR031204, 2022.
Kendall, M. G.: Rank correlation methods, Griffin, London1948.
Klingler, C., Schulz, K., and Herrnegger, M.: LamaH-CE: LArge-SaMple DAta for Hydrology and Environmental Sciences for Central Europe, Earth Syst. Sci. Data, 13, 4529-4565, 10.5194/essd-13-4529-2021, 2021.
Lane, E. W. and Lei, K.: Stream Flow Variability, Transactions of the American Society of Civil Engineers, 115, 1084-1098, doi:10.1061/TACEAT.0006394, 1950.
Lane, R. A. and Kay, A. L.: Climate Change Impact on the Magnitude and Timing of Hydrological Extremes Across Great Britain, Frontiers in Water, 3, 10.3389/frwa.2021.684982, 2021.
Lane, R. A., Coxon, G., Freer, J., Seibert, J., and Wagener, T.: A large-sample investigation into uncertain climate change impacts on high flows across Great Britain, Hydrol. Earth Syst. Sci., 26, 5535-5554, 10.5194/hess-26-5535-2022, 2022.

McMillan, H., Westerberg, I., and Branger, F.: Five guidelines for selecting hydrological signatures, Hydrological Processes, 31, 4757-4761, 2017.
Nearing, G. S., Kratzert, F., Sampson, A. K., Pelissier, C. S., Klotz, D., Frame, J. M., Prieto, C., and Gupta, H. V.: What Role Does Hydrological Science Play in the Age of Machine Learning?, Water Resources Research, 57, e2020WR028091, https://doi.org/10.1029/2020WR028091, 2021.
Olden, J. D. and Poff, N. L.: Redundancy and the choice of hydrologic indices for characterizing streamflow regimes, River Research and Applications, 19, 101-121, https://doi.org/10.1002/rra.700, 2003.
Paine, L.: River Cultures in World History—Rescuing a Neglected Resource, Fudan Journal of the Humanities and Social Sciences, 12, 457-472, 10.1007/s40647-018-0220-4, 2019.
Palmer, M. and Ruhi, A.: Linkages between flow regime, biota, and ecosystem processes: Implications for river restoration, Science, 365, eaaw2087, 10.1126/science.aaw2087, 2019.
Pettitt, A. N.: A Non-Parametric Approach to the Change-Point Problem, Journal of the Royal Statistical Society: Series C (Applied Statistics), 28, 126-135, https://doi.org/10.2307/2346729, 1979.
Poff, N. L. and Ward, J. V.: Implications of Streamflow Variability and Predictability for Lotic Community Structure: A Regional Analysis of Streamflow Patterns, Canadian Journal of Fisheries and Aquatic Sciences, 46, 1805-1818, 10.1139/f89-228, 1989.
Poff, N. L., Allan, J. D., Bain, M. B., Karr, J. R., Prestegaard, K. L., Richter, B. D., Sparks, R. E., and Stromberg, J. C.: The natural flow regime, BioScience, 47, 769-784, 1997.
Posavec, K., Bačani, A., and Nakić, Z.: A Visual Basic Spreadsheet Macro for Recession Curve Analysis, Groundwater, 44, 764-767, https://doi.org/10.1111/j.1745-6584.2006.00226.x, 2006.
Richter, B. D., Baumgartner, J. V., Powell, J., and Braun, D. P.: A Method for Assessing Hydrologic Alteration within Ecosystems, Conservation Biology, 10, 1163-1174, https://doi.org/10.1046/j.1523-1739.1996.10041163.x, 1996.
Rood, S., Mahoney, J., Reid, D., and Zilm, L.: Instream Flows and the Decline of Riparian Cottonwoods Along the St. Mary River, Alberta, Canadian Journal of Botany, 73, 1250-1260, 10.1139/b95-136, 1995.
Safeeq, M., Grant, G. E., Lewis, S. L., and Tague, C. L.: Coupling snowpack and groundwater dynamics to interpret historical streamflow trends in the western United States, Hydrological Processes, 27, 655-668, 2013.
Sauquet, E., Shanafield, M., Hammond, J. C., Sefton, C., Leigh, C., and Datry, T.: Classification and trends in intermittent river flow regimes in Australia, northwestern Europe and USA: A global perspective, Journal of Hydrology, 597, 126170, https://doi.org/10.1016/j.jhydrol.2021.126170, 2021.
Sawicz, K., Wagener, T., Sivapalan, M., Troch, P. A., and Carrillo, G.: Catchment classification: empirical analysis of hydrologic similarity based on catchment function in the eastern USA, Hydrology and Earth System Sciences, 15, 2895-2911, 2011.
Sen, P. K.: Estimates of the regression coefficient based on Kendall's tau, Journal of the American statistical association, 63, 1379-1389, 1968.
Shih, S.-S., Liu, C.-H., and Ning, J.-H.: In-river weir effects on the alteration of flow regime and regarding structural stream habitat, Journal of Hydrology, 615, 128670, 10.1016/j.jhydrol.2022.128670, 2022.
Singh, S. K., Pahlow, M., Booker, D. J., Shankar, U., and Chamorro, A.: Towards baseflow index characterisation at national scale in New Zealand, Journal of Hydrology, 568, 646-657, 2019.
Sun, A. Y., Jiang, P., Mudunuru, M. K., and Chen, X.: Explore Spatio-Temporal Learning of Large Sample Hydrology Using Graph Neural Networks, Water Resources Research, 57, e2021WR030394, https://doi.org/10.1029/2021WR030394, 2021.
Suzuki, K., Hiyama, T., Matsuo, K., Ichii, K., Iijima, Y., and Yamazaki, D.: Accelerated continental‐scale snowmelt and ecohydrological impacts in the four largest Siberian river basins in response to spring warming, Hydrological Processes, 34, 3867-3881, 2020.
Tan, A., Adam, J. C., and Lettenmaier, D. P.: Change in spring snowmelt timing in Eurasian Arctic rivers, Journal of Geophysical Research: Atmospheres, 116, 2011.
The Nature Conservancy: Indicators of Hydrologic Alteration Version 7.1 User's Manual, 2009.
Tonkin, J. D., Merritt, D., Olden, J. D., Reynolds, L. V., and Lytle, D. A.: Flow regime alteration degrades ecological networks in riparian ecosystems, Nature ecology & evolution, 2, 86-93, 2018.
Torabi Haghighi, A., Yaraghi, N., Sönmez, M. E., Darabi, H., Kum, G., Çelebi, A., and Kløve, B.: An index-based approach for assessment of upstream-downstream flow regime alteration, Journal of Hydrology, 600, 126697, https://doi.org/10.1016/j.jhydrol.2021.126697, 2021.
Tramblay, Y., Rouché, N., Paturel, J. E., Mahé, G., Boyer, J. F., Amoussou, E., Bodian, A., Dacosta, H., Dakhlaoui, H., Dezetter, A., Hughes, D., Hanich, L., Peugeot, C., Tshimanga, R., and Lachassagne, P.: ADHI: the African Database of Hydrometric Indices (1950–2018), Earth Syst. Sci. Data, 13, 1547-1560, 10.5194/essd-13-1547-2021, 2021.
Troin, M., Martel, J.-L., Arsenault, R., and Brissette, F.: Large-sample study of uncertainty of hydrological model components over North America, Journal of Hydrology, 609, 127766, https://doi.org/10.1016/j.jhydrol.2022.127766, 2022.
UKIH: Institute of Hydrology: Low Flow Studies Report No 3, Institute of Hydrology, Wallingford, UK, 1980.
Wasko, C., Nathan, R., and Peel, M. C.: Trends in global flood and streamflow timing based on local water year, Water Resources Research, 56, e2020WR027233, 2020.
Westerberg, I. K. and McMillan, H. K.: Uncertainty in hydrological signatures, Hydrol. Earth Syst. Sci., 19, 3951-3968, 10.5194/hess-19-3951-2015, 2015.
Worku, F. F., Werner, M., Wright, N., van der Zaag, P., and Demissie, S. S.: Flow regime change in an endorheic basin in southern Ethiopia, Hydrology and Earth System Science, 18, 3837-3853, 10.5194/hess-18-3837-2014, 2014.

Yang, Y., Roderick, M. L., Yang, D., Wang, Z., Ruan, F., McVicar, T. R., Zhang, S., and Beck, H. E.: Streamflow stationarity in a changing world, Environmental Research Letters, 16, 064096, 2021.

Yin, J., Gentine, P., Zhou, S., Sullivan, S. C., Wang, R., Zhang, Y., and Guo, S.: Large increase in global storm runoff extremes driven by climate and anthropogenic changes, Nature Communications, 9, 4389, 10.1038/s41467-018-06765-2, 2018.

Yin, Z., Lin, P., Riggs, R., Allen, G. H., Lei, X., Zheng, Z., and Cai, S.: A Synthesis of Global Streamflow characteristics, Hydrometeorology, and catchment Attributes (GSHA) for Large Sample River-Centric Studies, Earth Syst. Sci. Data Discuss., 2023, 1-36, 10.5194/essd-2023-256, 2023.

Zhang, S. X., Bari, M., Amirthanathan, G., Kent, D., MacDonald, A., and Shin, D.: Hydrologic reference stations to monitor climate-driven streamflow variability and trends, Hydrology and Water Resources Symposium,

Zhang, X. S., Amirthanathan, G. E., Bari, M. A., Laugesen, R. M., Shin, D., Kent, D. M., MacDonald, A. M., Turner, M. E., and Tuteja, N. K.: How streamflow has changed across Australia since the 1950s: evidence from the network of hydrologic reference stations, Hydrology and Earth System Sciences, 20, 3947-3965, 2016.